SAHC

Stability Analysis of St. Barbara Church in Otovice

Ivana Božulić

Czech Republic | 2019

ADVANCED MASTERS IN STRUCTURAL ANALYSYS
OF MONUMENTS AND HISTORICAL CONSTRUCTION

# Master's Thesis

Ivana Božulić

# Stability Analysis of St. Barbara Church in Otovice

University of Minho

**Czech Republic** | 2019



ADVANCED MASTERS IN STRUCTURAL ANALYSYS
OF MONUMENTS AND HISTORICAL CONSTRUCTION

# Master's Thesis

Ivana Božulić

## Stability Analysis of St. Barbara Church in Otovice

Czech Republic | 2019

**CZECH TECHNICAL UNIVERSITY IN PRAGUE**
**Faculty of Civil Engineering**
Thákurova 7, 166 29 Prague 6, Czech Republic

# MASTER'S THESIS PROPOSAL

study programme: Civil Engineering

study branch: Advanced Masters in Structural Analysis of Monuments and Historical Constructions

academic year: 2018/2019

Student's name and surname: Ivana Božulić

Department: Department of Mechanics

Thesis supervisor: Pavel Kuklík

Thesis title: Stability Analysis of St. Barbara Church in Otovice

Thesis title in English: see above

Framework content: The main goal of the thesis is numerical modeling and evaluation of load bearing capacity and stability of St Barbara Church in Otovice, Czech Republic.

The focus of the dissertation will be given to nonlinear material response of the structural materials and nonlinear analysis of structural stability and load bearing capacity of the main structural parts. Structural stability can be also affected by the footings and their degradation in time. This effect together with the soil-structure interaction will be considered.

Historical review, geometrical survey, visual inspection damage mapping were carried out in order to increase level of knowledge about the structure.

After this, micromodeling of different portion of the wall was performed, which allowed obtaining more accurate mechanical parameters to calibrate 3D model.

The 3D model made in ATENA, was used to study the influence of differential settlements on the structure. This could explain some cracks observed during in situ inspection and it could show possible future cracking patterns and degradation mechanisms.

In conclusion, recommendations on obtaining more precise information on geometry and material properties and on monitoring strategies were given.

Assignment date: 1/04/2019 Submission date: 8/09/2019

If the student fails to submit the Master's thesis on time, they are obliged to justify this fact in advance in writing, if this request (submitted through the Student Registrar) is granted by the Dean, the Dean will assign the student a substitute date for holding the final graduation examination (2 attempts for FGE remain). If this fact is not appropriately excused or if the request is not granted by the Dean, the Dean will assign the student a date for retaking the final graduation examination, FGE can be retaken only once. (Study and Examination Code, Art 22, Par 3, 4.)

*The student takes notice of the obligation of working out the Master's thesis on their own, without any outside help, except for consultation. The list of references, other sources and names of consultants must be included in the Master's thesis.*

| | |
|---|---|
| ..... | ..... |
| Master's thesis supervisor | Head of department |

Date of Master's thesis proposal take over: July 2019

.....
Student

This form must be completed in 3 copies – 1x department, 1x student, 1x Student Registrar (sent by department)

No later than by the end of the 2nd week of instruction in the semester, the department shall send one copy of BT Proposal to the Student Registrar and enter data into the faculty information system KOS. (Dean's Instruction for Implementation of Study Programmes and FGE at FCE CTU Art. 5, Par. 7)

# DECLARATION


| | |
|---|---|
| Name: | Ivana Božulić |
| Email: | Ivana.bozulic@gmail.com |


| | |
|---|---|
| Title of the Msc Dissertation: | Stability Analysis of St Barbara Church in Otovice |
| Supervisor(s): | Prof. Pavel Kuklik |
| Year: | 2018/2019 |

I hereby declare that all information in this document has been obtained and presented in accordance with academic rules and ethical conduct. I also declare that, as required by these rules and conduct, I have fully cited and referenced all material and results that are not original to this work.

I hereby declare that the MSc Consortium responsible for the Advanced Masters in Structural Analysis of Monuments and Historical Constructions is allowed to store and make available electronically the present MSc Dissertation.

| | |
|---|---|
| University: | Czech Technical University in Prague, Czech Republic |
| Date: | July 8th, 2019 |
| Signature: | _____ |

This page is left blank on purpose.

## ACKNOWLEDGEMENTS

First, I would like to express my gratitude to my supervisor, Prof. Pavel Kuklik, who guided me throughout my thesis with his expertise, patience, and kindness.

Many thanks to Prof. Petr Kabele for all his help, guidance, constant presence and diligence during our stay in Prague. Also, I would like to thank Prof. Kateřina Kovářová for sharing valuable information and suggestions with me.

Sincere gratitude to the SAHC Consortium for the scholarship they provided me without which I would not have been able to begin this amazing experience.

I am also thankful to all the professors from the University of Minho, Portugal for sharing their knowledge and passion for historical buildings during the coursework.

I gratefully acknowledge the support of Jacopo Scacco. I truly appreciate his advice, friendship and valuable feedback at times.

I am also grateful for the new friendships and amazing moments we shared during this unforgettable year. Without acquaintances who shortly became best friends, without all the laughs, trips, cafeteria breaks this unrepeatable year would not be the same.

Finally, I thank my family and friends for their constant support, love, and encouragement in all the possible ways.

This page is left blank on purpose.

## ABSTRACT

Broumov Region and its group of churches represent a perfect example of symbiosis between Baroque architecture and countryside landscape. This peculiar heritage site requires specialized analysis to preserve its uniqueness. St. Barbara Church in Otovice, the one investigated in this thesis, was built by Christoph and Kilian Dientzenhofer.

Nowadays, concerns about its stability and degradation process led to the necessity to investigate more deeply its current condition. Therefore, the main objective of the thesis consisted in the FEM modeling and the evaluation of the bearing capacity of enclosure walls, with particular attention on the influence of the soil deterioration.

The thesis, after a historical introduction, focused on a few damages experienced by the church and trials to define their possible causes.

After this, micro modeling of different portions of the wall was carried out using ATENA 2D. This approach allowed to obtain mechanical parameters, with values comparable to reliable standards, to be used afterward for the 3D model in ATENA 3D.

The information available for the soil properties allowed to determine the overall settlement of the structure, through simple elastic analysis with GEO5 and ATENA 3D. The values acquired with these two different approaches resulted to be similar.

After this, the nonlinear analysis explored different scenarios, studying the influence on the structure of possible future differential settlements. Moreover, a reasonable explanation of the currently cracking pattern is provided.

In conclusion, technical advice is recommended, along with monitoring strategies.

**Keywords:** Baroque, soil-structure interaction, bearing capacity, crack propagation, cultural heritage, stability.

This page is left blank on purpose.

## ABSTRAKT

**Analýzy stabilita z Kostel sv. Barbory v Broumovsko.**

Broumovsko a jeho skupina barokních kostelů představuje výjimečný příklad kombinace architektury a venkovské krajiny. Toto zvláštní dědictví vyžaduje speciální odbornou analýzu, aby byla zachována jeho jedinečnost. Kostel svatého Barbory, který byl zkoumán v této diplomové práci, byl vybudovali Kryštof a Kilián Dientzenhoferové.

Dnešní obavy, týkající se jeho stability a stavu degradace, vedly k nutnosti hlouběji prozkoumat jeho současnou situaci, která je ovlivněna řadou nejistot. Hlavním cílem práce byla tedy modelování MKP a následné vyhodnocení únosnosti stěn obvodového pláště se zaměřením na vliv degradace podloží.

Tato práce, po historickém úvodu, se zaměřila na vybrané poruchy, které jsou na kostele patrné, a stanovení jejich příčin.

Následně, bylo pomocí software ATENA 2D provedeno určité mikromodelování různých částí zdi. Toto řešení umožnilo získat mechanické parametry, jež jsou srovnatelné se spolehlivými normami. Tyto hodnoty byly následně použity pro 3D modelování užitím numerického kódu ATENA 3D.

Dostupné informace o vlastnostech podloží nám umožnily stanovit celkové sedání stavby pomocí elastické analýzy pomocí kódů GEO5 a ATENA. Získané hodnoty sedání pomocí obou kódů vykazovaly minimální odchylky.

Poté pomocí nelineární analýzy jsme prozkoumali různé scénáře zaměřené na nerovnoměrné sedání. Byl vytvořen určitý katalog možných poruch, který bude užitečný pro další analýzu. Mimo to se nám podařilo uspokojivě vysvětlit současný stav porušení prezentovaný sadou zjevných trhlin.

Na závěrem je navrženo technické opatření zaměřené na redukování nejistot současného stavu spolu se strategií sledování kostela.

**Klíčová slova:** Baroko, interakce stavby s podložím, únosnost, šíření trhliny, kulturní dědictví, stabilita.

This page is left blank on purpose.

# РЕЗИМЕ

**Анализа стабилности Цркве Свете Барбаре у Отовицама.**

Броумовски регион са својом групом цркава представља савршену симбиозу између Барокне архитектуре и руралног предела. Ово посебно место културног наслеђа захтева специјализовану анализу у циљу очувања своје јединствености. Црква Свете Барбаре, која је предмет испитивања ове тезе, саграђена је од стране Кристофа и Килијана Диценхофера.

У данашње време, забринутост око стабилности Цркве и процеса деградације, довели су до потребе за дубљим испитивањем ситуације. Стога, главни циљ тезе се састоји у МКЕ моделовању и процени носивости носећих зидова, са посвећеном посебном пажњом на утицај деградације тла.

После историјског увода, теза се фокусира на оштећења у Цркви, уз покушаје дефинисања њихових узрока.

Након овога, микромоделовање различитих делова зида је извршено уз помоћ софтвера АТЕНА 2Д. Овакав приступ омогућио је прикупљање механичких параметара, који су касније коришћени за калибрацију 3Д модела у АТЕНИ 3Д.

Подаци о карактеристикама тла омогућили су анализу укупног слегања конструкције, уз помоћ софтбера ГЕО5 и АТЕНА 3Д. Резултати добијени у ова два различита софтвера су упоредивог реда величине.

Потом, нелинеарном анализом истражено је више сценарија, узимајући у обзир могућа будућа слегања и њихове утицаје. Штавише, објашњења тренуте пропагације пукотина су дата.

У закључку, технички савети у циљу смањења броја непознатих фактора су предложени, као и препоруке у виду стратегија мониторинга.

**Кључне речи:** Барок, интеракција тло-конструкција, носивост, пропагација пукотина, културно наслеђе, стабилност.

This page is left blank on purpose.

## TABLE OF CONTENTS

## Table of Figures

List of Tables

# 1. INTRODUCTION

Broumov region in the Czech Republic represents one of the most valuable heritage sites of this country and Europe in general. Nine Baroque churches were built in the 18th century, after 30 Years War, by the famous family of Baroque architects Dientzenhofers.

The goal of this thesis is a nonlinear numerical evaluation of load bearing capacity and stability of St Barbara Church in Otovice, a significant witness of the Czech history.

In Czech Republic, the problem of deterioration of materials due to lack of maintenance is common, especially in the religious objects, that are not in use anymore. The geometrical survey, visual inspection, and damage mapping will be conducted on-site, with pointing out the deterioration mechanism and their severity level. Moreover, nondestructive tests, employing Schmidt Hammer and a thermographic camera, will be conducted.

The capacity of the enclosure wall will be examined by using different approaches of modeling in FEM software ATENA. For instance, the values acquired from the micromodel will be used to calibrate the 3D model of the Church, so the obtained results are more accurate.

Special attention will be paid to the soil-structure interaction since shallow foundations could have a major role in the stability of the Church. Nonlinear behaviour of the structure, due to differential settlements will be checked, as well as their influence on the crack propagation.

In conclusion, recommendations about decreasing the number of uncertainties and monitoring techniques will be provided.

.

This page is left blank on purpose.

# 2. HISTORICAL OVERVIEW

Before performing in situ investigation and further analysis of the Church, it is highly important to understand the origin of the building, in which historical circumstances it was built and in which architectural style. Moreover, knowledge about past times can help us to determine the materials and techniques used for construction as well as structural systems applied and possible issues that occurred during the lifetime of the Church.

## 2.1 History of Bohemia

The largest historical region of the Czech lands that is included in today's Czech Republic is Bohemia (Figure 2.1). It was named after the Boii, Celtic tribe that was constantly migrating inside the Roman Empire. In the 6th century, Slavic tribes arrived from the east, and their language slowly replaced the older Germanic and Celtic languages.


Figure 2.1. Map of Czech Republic

Christianity first appeared in the early 9th century, but it took several centuries to become a dominant religion. At that time, Bohemia was a part of Great Moravia, but after the death of the ruler, Svatopluk I, it came under the rule of the Přemyslid dynasty, who remained rulers for the next several centuries. The Přemyslid dukes Vratislav II (1058) and Vladislav II (1158) proclaimed themselves as "King of Bohemia", but their descendants returned to the title of duke.

The first King of Bohemia that was also chosen as Holy Roman Emperor was Charles IV, who became King in 1346. Under his reign, Bohemia reached its peak, both politically and economically. Prague became known as the intellectual and cultural center of Central Europe. Also, King Charles IV rebuilt Prague, established Nové Město, he founded Charles University in Prague and started with the construction of the bridge spanning two shores of Vltava river in Prague.

After the Battle of Mohacs, in 1526, Bohemia became a part of the Habsburg Monarchy.

At the beginning of the 17th century, a war between various Protestant and Catholic states was initiated when new Holy Roman Emperor, Ferdinand II, tried to impose religious uniformity, obliging people on

Roman Catholicism. The resulting Bohemian Revolt by Protestants in Bohemia led to the Thirty Years' War (1618-1648). This unfortunate event destroyed the entire region and resulted in a high reduction in a number of population.

At the end of the 18th century, a strong initiative to regain the Czech language as the language of administration, instead of German, started, but without any success, as well as the requests for the autonomy of Bohemia in the Habsburg Empire in 1848. Moreover, the Czech attempt to create Austria-Hungary-Bohemia monarchy failed in 1871. After World War I, Bohemia was the basis for a newly formed country of Czechoslovakia. After World War II, the country was lead by the Communist Party and politically turned to the Soviet Union. Also, Bohemia stopped to be an administrative region of Czechoslovakia, as the country was not divided in accordance to historical borders anymore. After the end of Czechoslovakia in 1993, Bohemia remained in the Czech Republic, where it is nowadays. [1]

## 2.2 Bohemian Baroque

The victory of the Catholics in the Thirty Years' war allowed the entrance to the new architectural style - Baroque, which filled the town with large palaces and flamboyant churches that were designed to impress. After The War, the Catholic upper class strongly supported the arrival of a new style, as it was the symbol of the power of the only legal church at that time. A new architectural trend provided new appearance to the Czech architecture. The name of Baroque came from the Portuguese word "Barocco" which means irregular stone or pearl but also refers to an idiom reflecting religious disturbances at that time.

Buildings erected in the first period are classified as Early Baroque, and they were usually designed by Italian architects, who brought Baroque from its cradle - Italy. The original Radical Baroque, that was created in Italy by Francesco Borromini and Guarino Guarini, was developed in Bohemia by father and son Dientzenhofer and Jan Blazej Santini-Aichel.

The first Baroque building in Central Europe was Wallenstein Palace (Valdštejnský palác) designed by Italian architects Giovanni Pieroni and Andrea Spezza. [2]

Figure 2.2. Wallenstein Palace

The first Baroque church built in Prague was The Church of Our Lady Victorious in the Lesser Town (Figure 2.3), which was originally built in Renaissance style, but during the war, it was rebuilt in the early Baroque style.

Figure 2.3. The Church of Our Lady Victorious in Prague

The next phase of this style, known as High Baroque occurred between 1690 and the middle of the 18th century. The most significant architects were a father and son Dientzenhofer, whose style was called “Radical Baroque” and it was based on the movement which was gained through curved walls and intersected oval spaces. In general, Baroque tends to evoke different emotional states, often in dramatic ways contrary to the previous styles, which tried to capture man’s ratio. Some of the characteristics commonly associated with this style are movement, grandeur, richness in decorations, a mixture of repetition and distortion of Classical motifs, etc. Architects were encouraged to implement new forms using light and shadows in dramatic intensity, to make a strong impression on people of the Church’s domination and protection.

Figure 2.4. Church of St John of Nepomuk in the New Town in Prague (left) and The interior of St Nicholas Church in the Lesser Town in Prague (right)

## 2.3 Broumov Region

Broumov region is situated in the northeast of the Czech Republic, near the border with Poland. As an integral part of Bohemia, this region endured difficult events throughout its history and managed to stay a safeguard of cultural values. The region is precious due to its baroque monuments that are of high architectural and religious importance.

Broumov was first mentioned in documents in 1256. Benedictine monks of Břevnov Abbey in Prague began to colonize the lands in 1213. It became a center of textile manufacturers with the sales market all over Bohemia and Silesia. In 1348, King Charles IV granted privileges for the town of Broumov as the administrative centre of the abbey's manors. [3]

The city layout is still preserved as the original Silesian type of town, with typical main streets connecting the whole built-up area and gates located on the opposite sides of the town. In 1357, the construction of city walls started and, with great difficulties and expenses, it finished in 1380. Moreover, after a huge fire, in the 14th century, the monastery and church dedicated to St.Adalbert (St. Vojtech) were built on the site of former citadel. This information strongly suggests that Broumov was one of the most important centers in Bohemia in the 14th century. During the 16th century, the conflict between Catholics and Protestants left a mark on this region. It was named The Thirty Years' War due to its duration (1618-1648) and as it was mentioned, it ended with a victory of the Catholics, promising brighter future to the Benedictines.[4]

The twentieth-century was not very fortunate for this region. After World War II and the new country politics, the imposed atheism led to neglecting of churches. Moreover, the number of inhabitants was highly reduced after the war. The reason of the current damaged state for the buildings, due to the lack of maintenance, can be found in these facts.

## 2.4 Broumov Churches and Dientzenhofer Family

Broumov territory landscape was influenced by the prominent abbots, such as Tomáš Sartorius (1663−1700) and Otmar Zinke (1700−1738) and their construction works. At the end of the 17th century, Martin and Giovanni Battista Allios started with building new churches in the Broumov region (Figure 2.5).

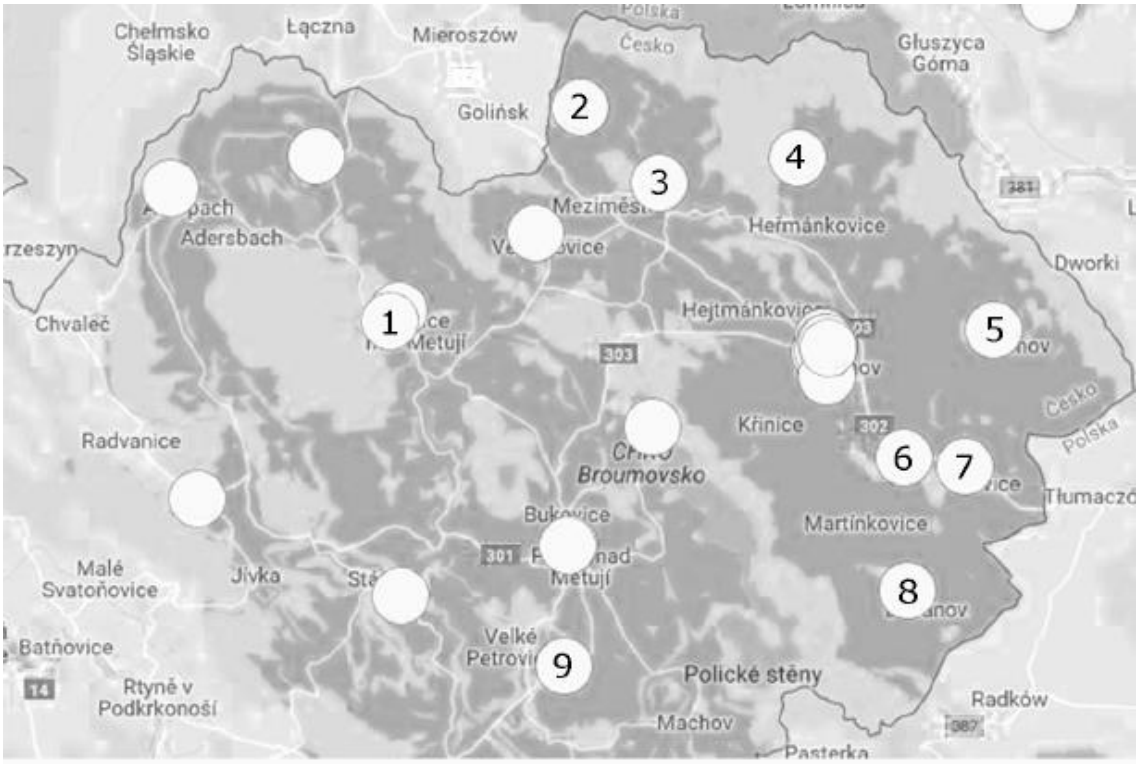


Figure 2.5. Map of Broumov Churches

An extremely important contribution to the development of the Czech Baroque style was given by Christoph and Kilian Ignaz Dientzenhofer (father and son) [5]. Christoph Dientzenhofer was a respected Bavarian architect, coming from the famous Dientzenhofer family of architects and he was known for using simple geometrical shapes, such as helix, with rhythmical curves.[5] Among his most famous works are the Church of St Nicholas in Prague (that was finished later by his son, Kilian) and the Brevnov Monastery in Prague (Figure 2.6).

Figure 2.6. Brevnov Monastery in Prague

After 1709, Christoph Dientzenhofer was involved in the reconstruction of the Broumov monastery and he designed St Michael Church in Vernéřovice (1719−1721) and St James in Ruprechtice (1720−1723) (Figure 2.7).

Figure 2.7. St Michael Church (left) and St James Church (right)

The other churches in Broumov region were work of his son, Kilian Ignaz Dientzenhofer, and they include: All Saints Church in Heřmánkovice (1723), St Anne Church in Vižňov (1725−1727), the extension of the presbytery by the church of St John the Evangelist in Janovičky (1725), St Barbara Church in Otovice (1725−1726), St Margaret Church in Šonov (1726−1730) and the Church of St Mary Magdalene in Božanov (Figures 2.8 and 2.9)

Figure 2.8. All Saints Church (left) and St Anne Church (right)

Figure 2.9. St Margaret Church (right) and St Mary Magdalene (right)

Kilian Ignaz Dientzenhofer was one of the leading Bohemian Baroque builders and he completed his father's work on the St Nicholas Church in Prague and among other works, it is worth mentioning that he designed Kinsky Palace in Prague (Figure 2.10)[6]. Kilian's work is recognized as much more dynamic with the curvatures in floor plans and plenty of details.

Figure 2.10. Kinsky Palace

In addition, the Broumov region is abundant with sandstone that was formed during the Mesozoic and Cretaceous period, when the sea entered the basin depositing calcareous clay which leads to the formation of the actual sandstone. This type of stone is extensively used in the construction of Broumov Churches.[5]

All the churches in the Broumov region were constructed similarly, with a single-nave ground plan, cheap and fast construction and simple decorations. Christian Norberg-Schulz mentioned in his article that the details of these churches are less accurate than in the other works of the same architects, probably due to economic problems. In the 19th century, some of the churches were renovated and adapted to meet the new needs of users.

Historical context, Baroque style, quantity, and quality of churches are what define *genius loci* of and make the Broumov region highly important and culturally valuable.

# 3. SAINT BARBARA CHURCH

St Barbara's Church (Figure 3.1) is a Roman Catholic church in Otovice and it belongs to the Broumov group of baroque churches. It is listed as a cultural monument in the Czech Republic. Some documents confirm the existence of an earlier wooden church consecrated to Saint George at the same place. The construction of a new church started in 1725, following the original draft of Christoph Dientzenhofer, but it was modified by his son, Kilian Ignaz. The main building phase happened in 1726. Between 1748 and 1750, there were still works on the design of the interior. [7]

Figure 3.1. St Barbara Church

## 3.1 Architectural Features

The single-aisle church has oval (longitudinal ellipse) shape with seven semicircular chapels including a chancel. It is 22m long and 15 m wide. The height of the church is 15.5m, measured from the floor to the ceiling. The interior is divided by eight pilasters without feet [8]. Robust walls are the main structural elements and they transfer roof loads to the foundations and further to the ground. The walls are made of three leaves. Coring was not performed, due to the importance of the building, but it is assumed that the infill layer is made of rubble and is of poorer quality than external leaves.

The main entrance is in a flat western facade with a triangular gable. The protrusion above the entrance is rectangular with rounded corners. A timber frame supports the balcony where the organ is placed. Furthermore, the hallway has a conical ground plan. The church is covered with a wooden plastered ceiling imitating a flattened dome [9]. Instead of masonry vault, the timber ceiling was designed allowing the reduction of horizontal thrust on the enclosure walls leading to the thinner walls.

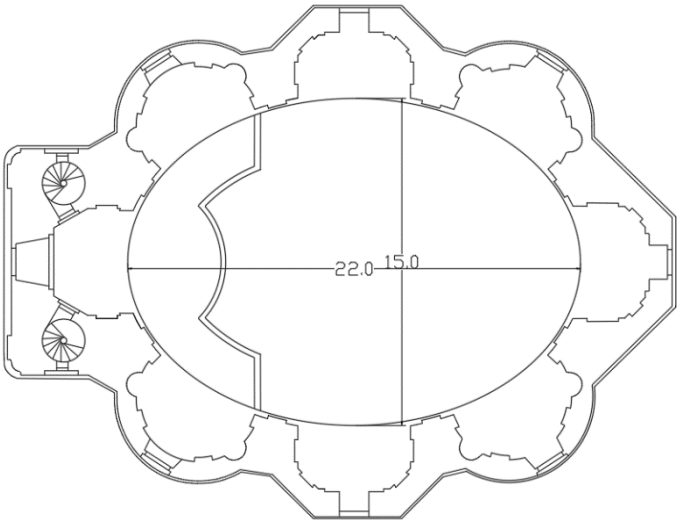


Figure 3.2. Floorplan of St Barbara Church

Externally, the church appears picturesque as a result of the curved contour due to the semicircular chapels. The structure is designed with a steep roof, which allows snow and rain to run off quickly. A roof truss is extremely complex, as it can be seen in Figure 3.3. The stability of the roof truss is improved by using St Andrew's cross. Originally, it was made of red-painted wood to finally be replaced by the more durable slate. The facades were covered by colored renderings due to weathering and economic costs.

Figure 3.3. Roof truss in the Church

Even today, above the main entrance, there is a plaque with the initials of Abbot Otmar Zinke and the year when St Barbara Church was consecrated - 1726. The church has no tower, only a small slipper. Nowadays, the only interior furnishing is altar structure, which originally was probably the most valuable part of the church as it preserved a rarely late Gothic and Renaissance paintings and sculptures. These precious items are safely stored in the Broumov Museum.

## 3.2 Materials

Traditional building materials depend significantly on local culture and availability. Masonry was usually chosen as a building material because it is durable and resistant and simple to manufacture. In order to make an accurate model and to understand the principles of behaviour, the characterization of materials was needed.

*Walls and foundation*

Materials used in the construction of this church are mostly from the local quarries in the surrounding area. Sandstones are mainly used since the Broumov region is abundant in this type of stone.

As a result of the detachment of render, partial arrangements of the stones are visible, providing us knowledge about the bond and different materials that were used. Non-destructive testing was done in situ, (Schmidt Hammer and thermographic camera), for the sake of the identification of mechanical properties of the different stones. Grey sandstone, mudstone, and brick were mainly used. Joints are filled with lime mortar.

*Roof and ceiling*

Roof construction and ceiling were made completely of timber. The ceiling was covered by gypsum and lime plaster. From the outside, the roof is covered with metal sheets, which is probably due to the cheap recent intervention.

## 3.3 Soil Overview

Borehole testing was performed in two spots up to 12 meters, in front of the Church and behind it (as it can be seen in Figure 3.4) to fully identify soil and foundation conditions of St Barbara Church. This information was fundamental for the understanding the possibility of soil settlements and thus, the potential unfavourable stress state in the bearing walls and the propagation of the cracks.

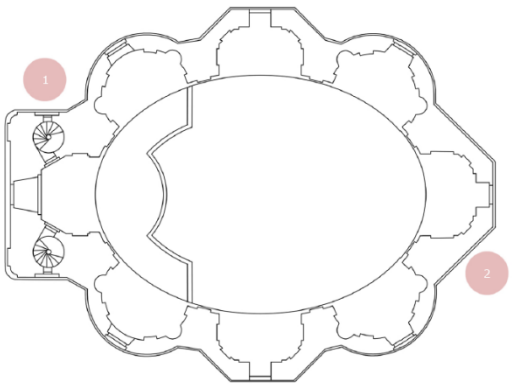


Figure 3.4. Locations of boreholes

## 3.4 Masonry Quality Assessment

Since only Schmidt Hammer in situ test was done, qualitative criterium was also used to assess the masonry quality. The Masonry Quality Index (MQI) allows evaluating whether a historic masonry wall was built according to the “rule of the art”, by identifying the presence of certain parameters. To calculate the MQI, seven parameters are taken into account.

$$MQI = SM\ (SD+SS+WC+HJ+VJ+MM)$$

**SM** stands for Conservation state and mechanical properties of the units, **SD** depends on the units dimension properties, **SS** refers to the shape of units, **WC** to the wall leaf connections, **HJ** and **VJ** describe vertical and horizontal joints characteristics, and **MM** depends on the Mortar mechanical properties. Each parameter is graded as fulfilled, partially fulfilled or not fulfilled. Moreover, the assessment depends on the type of loading of the wall.

Figure 3.5. Uncovered wall facade

Obtained values of different parameters are listed below:

SM=0.7; SD=0.5; SS=1.5; WC=1; HJ=1; VJ=0.5; MM=0.5 ⇒ MQI= 3.5 giving Category B meaning **Average** quality of masonry.

This approach depends on the engineer who is evaluating it, so results should be considered with attention.

# 4. DAMAGE SURVEY

In order to understand the existing condition of the Church structure, a damage survey was conducted. Such survey permitted the assessment of the most common deterioration mechanisms found at the church and the level of degradation of some of the structural systems and materials. Furthermore, the thermographic camera was also used, to determine areas with moisture issues and to understand better the configuration of the roof above the ceiling. In general, the Church seems to be in a fair condition thanks to the previous interventions that improved the drainage system. The location of damages, as well as their cause, will be further discussed in the report. Furthermore, comparison of condition with other churches from the region will be provided, when possible. The survey was carried out according to ICOMOS - Illustrated glossary on stone deterioration patterns.

Most of the observed damages can be linked to the lack of maintenance of the church due to different causes. Decreased number of inhabitants in the Broumov region, low numbers of Catholics and lack of economic assets led to the low level of maintenance and furthermore, most of the damages that can be seen on site.

Damage maps can be observed in Appendix A.

## 4.1 The exterior of the Church

The global condition of the exterior of the Church can be seen in Figure 4.1. In comparison with the other churches from the Broumov region, the Church of St Barbara shows a very well arranged course of stones, insignificant loss of material and good drainage system, resulting in a very good overall condition.

Figure 4.1. Facades of St Barbara Church (left) and St Anna Church (right)

*Cracks and deformations*

In the facade of the church, no significant cracks were observed. However, in the front door, a typical crack in the middle of the lintel can be noticed. Further damage was stopped by using a clamp.

Figure 4.2. Crack in the lintel

Cracks due to the soil settlements can be observed in few places, where foundation stones seem to be moved horizontally or diagonally.

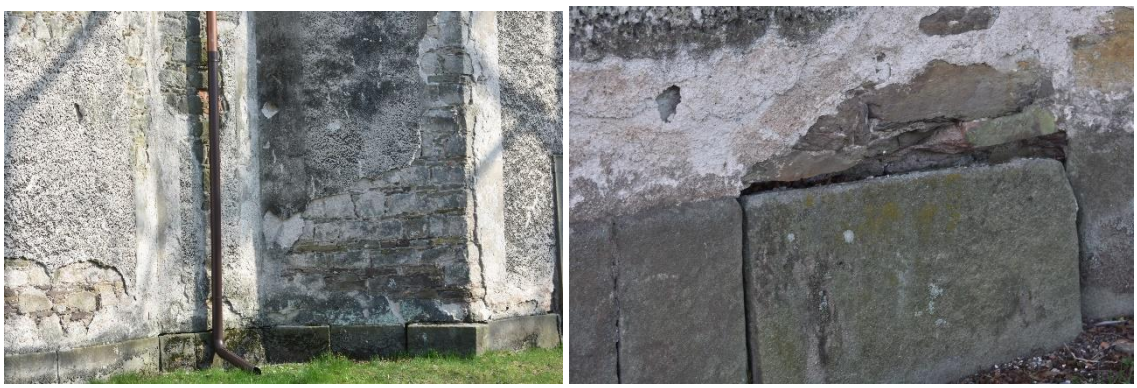

Figure 4.3. Cracks due to soil settlements

*Detachment*

The detachment of the plaster can be seen in multiple parts of the facade. Spalled render leaves the surface of stones unprotected, which can lead to further damage due to the weathering. The reason for this common phenomenon can be related to the presence of water, and its influence was reduced by the newly placed drainage system in the church.

Figure 4.4. Detachment of render

*Material Loss*

Due to weathering, the condition of the facade is not uniform, and the damage due to erosion can be seen. As a result of erosion, different stones deteriorate irregularly. Usually, only the stone surface is deteriorated, but the substrate is still sound. This phenomenon can be easily seen wherever the plaster is detached.

Figure 4.5. Material Loss

*Discoloration & Deposit*

The dark coloured crust can be observed mostly at the top of the church, in the areas that are protected against direct rainfall or water runoff. Black crust adheres firmly to the stone. It is mainly composed of atmospheric particles and its thickness is not constant.

Figure 4.6. Black crust

Furthermore, soiling, which is defined as a thin layer of atmospheric particles, giving a dirty appearance to the surface, is noticed in multiple spots on the facade. The substrate structure does not seem to be affected.

Figure 4.7. Soiling

Efflorescence is observed mostly at the bottom part of the structure, in the area of rising damp, where the humidity level is higher compared to the other parts of structures. Soluble salt crystals can be seen on the surface of the stone, and they are poorly bonded to it.

Figure 4.8. Efflorescence

*Biological colonization*

Biological colonization was found on the stones which are in contact with the ground, meaning the higher level of humidity allows creation of algae, lichens, and plants.

Figure 4.9. Biological growth

In conclusion, the main problem that was noticed is the loss of plaster's integrity and exposure of the stones to the weathering. Plaster is missing in different locations in the facade, but the decay is lower than in the other churches, probably due to the good drainage system. The reason for the common detachment is linked to the presence of water, both from the soil and from the roof. Gutters seem to be in good condition, allowing water to be taken away from the church, and thus, reducing the risk of foundation damage. The effects of soil settlement will be included in structural analysis and the results will be presented in the next chapters.

## 4.2 Interior of the Church

The overall condition of the interior of the Church is fair to good and much better than in St Anna Church and St Jacob Church. Most of the damage from water infiltration is avoided due to the new drainage system.

*Cracks and deformations*

On the ceiling, cracks with the regular patterns were observed. Their origin is probably related to the false vault system used in the Broumov group of churches since the same cracks were also detected in St. Jacob Church. Development of cracks occurred probably due to the long term actions and deformation of timber elements in roof trusses.

Figure 4.10. Cracks in the ceiling

Cracks located above windows could be related to the soil settlement phenomena, and this hypothesis will be further developed in Chapter 7.

Figure 4.11. Crack in the arch above the window

Microcracks in plaster can be seen all around the Church and probably their origin is connected with shrinkage of plaster.

Figure 4.12. Hair cracks in plaster

Moreover, some of the cracks can be related to the local concentrations of stresses.

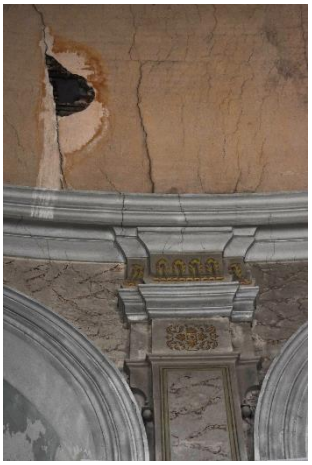

Figure 4.13. Cracks above pillar due to the concentration of stress

*Discoloration and deposit*

The level of rising damp is not very high and neither efflorescence nor subflorescence was observed in significant quantity. Also, visual inspection of the Church was carried out in April, during a sunny period. Humidity levels should be checked also for different weather conditions.

Locally, parts of plaster are detached and it can be seen that previous similar damages were treated during past interventions. During these repairs, applied plaster was based on cement, which is not the best solution for masonry walls, due to the low compatibility of properties.

Figure 4.14. Discoloration due to previous interventions and humidity level

Stains on the plaster on the ceiling were noticed, most likely due to the water infiltration. Different levels of this damage were noticed. The ultimate stage of this damage is a hole in the ceiling, which could lead to even worse deterioration.

Figure 4.15. Humidity stains on the plaster

*Biological colonization*

No significant signs of biological colonization were noticed inside the Church.

# 5. BEARING CAPACITY OF THE ENCLOSURE WALLS

Masonry structures were primarily built to sustain compression loads due to the usually negligible tensile strength of masonry. Therefore, through the empirical approach, masons developed shapes of constructive elements to support the weight of the building and vertical loads by compression only. Since the existing masonry structures show nonlinear behaviour even for the low levels of loading, it is necessary to use finite element analysis to compute the maximum load-bearing capacity of the enclosure walls.

First, the Finite Element Analysis was carried out for a 2D section of a wall, and afterward, with accurately obtained parameters of masonry walls, FEA was performed on the 3D model of the Church.

## 5.1 2D Model

The lack of information on geometry, material properties, techniques used for initial construction as well as reconstructions done over the service life of an existing building cause difficulties in accuracy in numerical modeling. Furthermore, nonregular arrangement of the stones makes application of any standard inaccurate. Thus, in order to obtain more precise properties for the calibration of the 3D model, the “micromodeling” approach was used.

According to the photos taken on-site, the FE model was made to represent the current condition of the walls. Wall was made of different types of locally abundant stones, bonded together with lime mortar. In order to obtain the accurate “micromodel”, blocks of sandstone, mudstone, bricks, rubble, and lime mortar were applied with their specific mechanical characteristics, gathered during *in situ* testing or taken from literature.

## 5.2 Modeling Assumptions

Material properties of the masonry are derived from its composite nature. Compressive strength of a unit, especially in the case of stone blocks, is usually significantly higher than one of the mortar. Therefore, the compressive strength of the masonry as a composite is derived from the value of both constituents. In order to obtain these values, nondestructive in situ testing by using Schmidt Hammer was carried out.

The composite behaviour results from different mechanical parameters governing the deformations of the units and the mortar. Under the compression, orthogonal deformation of unit and mortar is distinct due to different stiffness and Poisson coefficient. In the majority of the cases, units are stiffer component and mortar tends to have larger orthogonal deformations. Incompatibility of deformations causes shear stress in the interface which can lead to cracking. However, for the sake of modeling simplicity, the interface is assumed to be rigid. This hypothesis can be partially justified with the fair interlocking between stones and mortar, due to the friction (rough surfaces). For the purpose of determining the behaviour curve (stress vs deformation), the simulation of the double flat jack test in finite element

software was carried out. This allowed the estimation of the elastic modulus of the wall as well as load capacity.

Modeling of two longitudinal and two sectional parts of the wall was performed. Two steel plates, with a thickness of 10 cm, were modeled at the top and the bottom of the specimen in order to redistribute the applied load. The load was assigned as a prescribed displacement of 0.5 mm in each step. Boundary conditions applied in the bottom line of steel plate restricted movements in both x and y-direction. The hypothesis of plane stress was assumed for longitudinal walls, and plain strain for sectional ones.

Newton-Rhapson method was used for nonlinear calculation, along with line search. The iteration limit was assigned as 30.

## 5.3 Surface Hardness Testing

External parts of the walls with detached render served as testing locations. In order to have more accurate results, testing was performed on two different parts of the enclosure walls, the first one located in the facade wall, and the other in the longitudinal wall. Data from these spots were used in further analysis, as it can be seen in Figure 5.1. In order to obtain the surface hardness, which can yield the useful value of the superficial strength of different stones, the non-destructive Schmidt Hammer test was performed. In Figure 5.1 and Table 5.1 detailed drawings of the testing spots in the external leaf of the wall, as well as results obtained by Schmidt Hammer campaign, can be observed. The main disadvantage of this method is that it represents only a 5cm deep layer and does not provide the information on the characteristics of a whole volume of element. Moreover, the obtained data is very sensitive to the presence of moisture and it is important to be careful with the application of these results. In each sample, three different types of stone were noticed, as well as the deteriorated units on which the test could not have been carried out. The rebound test was performed 15 times on each stone, and then Schmidt Hammer provided results of the average value of the rebound number and Standard Deviation.

Figure 5.1. Two different parts of the enclosure walls that were tested

Table 5.1. Schmidt Hammer testing results

| | 1 | | | 2 | | |
|---|---|---|---|---|---|---|
| Hits | A | B | C | A | B | C |
| 1 | 25.0 | 21.0 | 50.5 | 14.5 | 34.5 | 50.5 |
| 2 | 36.0 | 27.5 | 49.0 | 17.5 | 28.0 | 46.0 |
| 3 | 33.5 | 37.5 | 44.0 | 18.5 | 24.5 | 54.5 |
| 4 | 36.5 | 27.5 | 54.5 | 14.5 | 38.5 | 48.0 |
| 5 | 41.0 | 33.5 | 51.0 | 14.5 | 39.5 | 46.0 |
| 6 | 39.0 | 28.5 | 44.5 | 22.5 | 30.0 | 47.5 |
| 7 | 37.0 | 34.0 | 51.5 | 18.5 | 30.5 | 44.5 |
| 8 | 28.5 | 37.5 | 53.5 | 19.5 | 32.0 | 48.0 |
| 9 | 31.5 | 35.0 | 44.5 | 22.5 | 40.5 | 46.5 |
| 10 | 41.0 | 40.0 | 47.5 | 20.0 | 46.0 | 48.0 |
| 11 | 34.5 | 39.5 | 50.5 | 17.5 | 34.5 | 38.0 |
| 12 | 19.5 | 33.0 | 57.0 | 20.0 | 33.0 | 33.5 |
| 13 | 43.5 | 32.5 | 48.5 | 20.0 | 33.5 | 37.5 |
| 14 | 18.0 | 38.5 | 59.5 | 21.0 | 37.5 | 32.0 |
| 15 | 37.5 | 35.0 | 50.5 | 18.0 | 39.5 | 31.5 |
| | | | | | | |
| Average Q | 33.5 | 33.4 | 50.4 | 18.6 | 34.8 | 43.5 |
| S | 8.5 | 5.3 | 4.4 | 1.6 | 5.5 | 7.1 |
| $f_{ck}$ [Mpa] | 17.0 | 16.5 | 49.5 | 20.0 | 18.0 | 31.0 |

Regarding obtained results, apart from the average value of Q and Standard Deviation, the value of compressive strength was also calculated automatically, by the Schmidt Hammer. This transformation was calculated by the formula provided by the manufacturer of the equipment (Proceq, 2017).

$$f_c = 0{,}0108Q^2 + 0{,}223Q$$

In Figure 5.2 below, grey sandstone is shown in blue (B), bricks are red (C) and mudstone is orange (A). The same notation was used in Table 5.1.

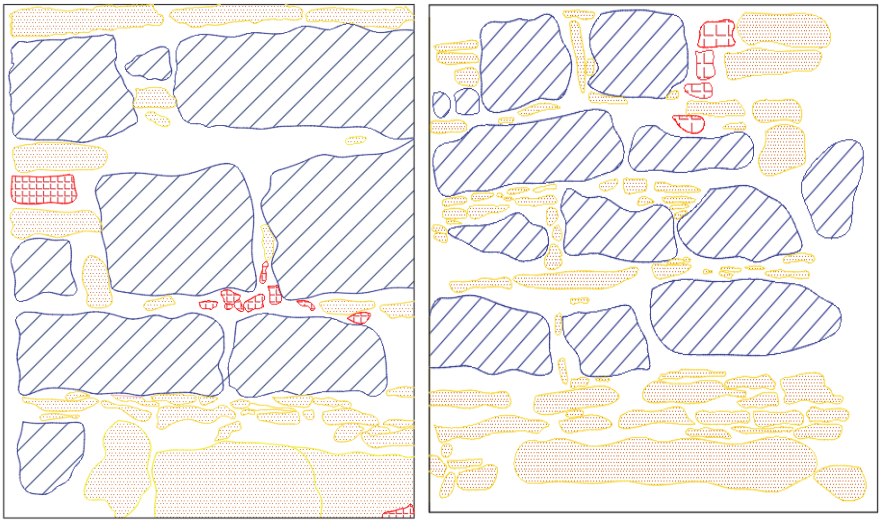

Figure 5.2. AutoCAD drawing of wall sections

## 5.4 Material Properties

Software ATENA 2D was used for the modeling of the sections of the walls. Longitudinal and sectional walls were analysed separately. Masonry walls in existing buildings are usually three-leaf walls, with rubble infill. Collected information *in situ* was related only to the external leaf, but these results were assumed also for the internal leaf. Moreover, the minimal value of the compressive strength obtained by Schmidt Hammer was chosen, which represents a conservative approach. Tensile strength was calculated as 1/10 of compressive strength. Other material properties were obtained from the literature [10] and the Italian Code [18].

Table 5.2. Material Properties

| | E [GPa] | v | fc [MPa] | ft [MPa] | Gt [N/m] | $\varepsilon_c$ | ρ $[kN/m^3]$ |
|---|---|---|---|---|---|---|---|
| Grey sandstone | 13 | 0.2 | 20 | 2 | 58 | 0.0015 | 21 |
| Bricks | 5 | 0.2 | 18 | 1.8 | 52.2 | 0.0036 | 19 |
| Mudstone | 9.21 | 0.2 | 48 | 4.8 | 50 | 0.0015 | 20 |
| Lime Mortar | 0.125 | 0.2 | 1.1 | 0.11 | 10 | 0.0217 | 17.8 |
| Rubble | 0.7 | 0.2 | 2 | 0.05 | 10 | 0.0029 | 20 |
| Steel plates | 200 | 0.3 | - | | - | - | 0 |

## 5.5 Material Constitutive Model

While working in the software that is mainly dedicated to the reinforced concrete, special attention has to be paid to the modeling of the masonry. The selected constitutive model was “Non-Linear Cementitious 2”. This plastic model merges the constitutive models for tensile (fracturing) and compressive (plastic) behaviour. The fracture model is based on the orthotropic smeared crack formulation and crack band model [11]. The smeared approach means that the damaged material is still considered as a continuum [12]. This material model assumes a hardening regime before the compressive strength is reached, with purely incremental formulation, thus this material model can be used when it is necessary to change material properties during the analysis [11]. Also, in this material model, tensile behaviour is described by an exponential opening law which requires the definition of the fracture energy in tension (Figure 5.3).

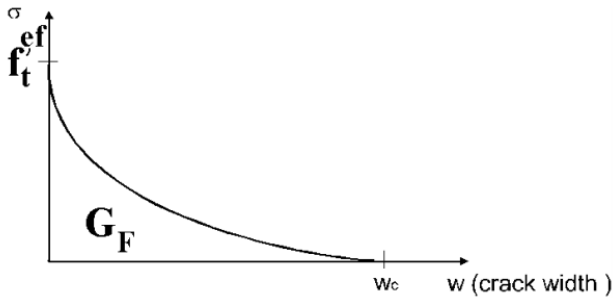


Figure 5.3. Exponential crack opening law [11]

This function was experimentally obtained by Hordijk (1991).

$$\frac{\sigma}{f_t^{'ef}} = \left\{1+\left(c_1\frac{w}{w_c}\right)^3\right\}\exp\left(-c_2\frac{w}{w_c}\right)-\frac{w}{w_c}\left(1+c_1^3\right)\exp\left(-c_2\right),$$

$$w_c = 5.14\frac{G_f}{f_t^{'ef}},$$

where w is the crack opening, $w_c$ is the crack opening at the point of complete release of stress and σ is the normal stress in the crack. Gf is the fracture energy needed to create a unit area of the stress-free crack. This softening law is based on the dissipated energy.

In the case of compression, failure, as well as all post-peak compressive displacements and energy dissipation, are localized in a plane normal to the direction of compressive principal stress. The endpoint of the curve is defined by the plastic displacement $w_d$ and this indirectly defines the energy needed for the generation of a unit area of the failure plane. Moreover, the strain at the peak stress had to be determined.

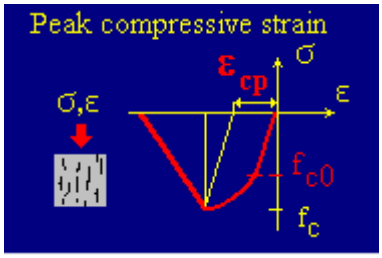


Figure 5.4. Peak compressive strain [11]

For the 2D model, a fixed crack model was used.

### 5.6 Longitudinal Wall

Two different parts of the wall of the Church were examined in situ and modeled in ATENA 2D. Assessed area of the wall was 1m x 0.8m in one case, 1m x 1m in another, which are also the dimensions of the models. The setups of walls are mostly realistic, with simplification due to the meshing of a model. Simplification of the setup was necessary, but still the corners of polygonal objects can show unrealistic results, due to the concentration of stresses in corners. Due to the meshing issues, sharp angles in the model were avoided. The mesh size is set as 2 cm. Different material properties were assigned to each type of stone. The steel plates were modeled at the bottom and the base of the specimen, allowing the equal distribution of the loads. The applied load was the imposed displacement of 0.5mm for each step.

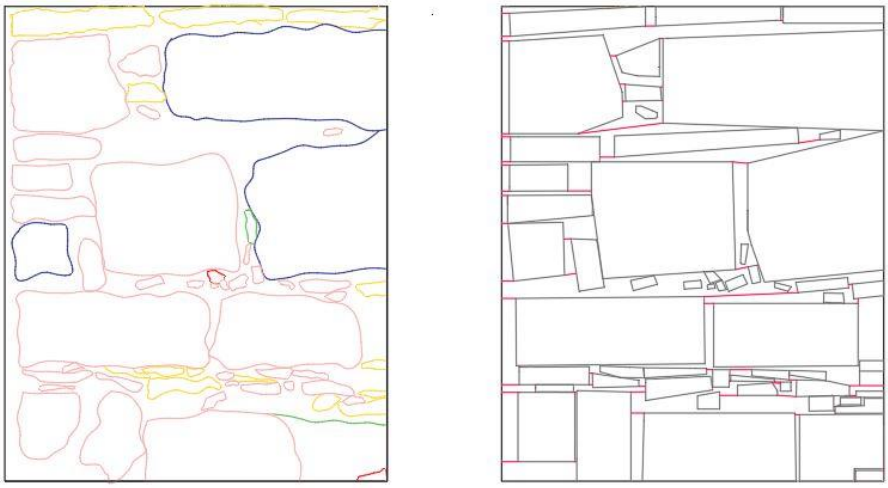

Figure 5.5. Facade wall

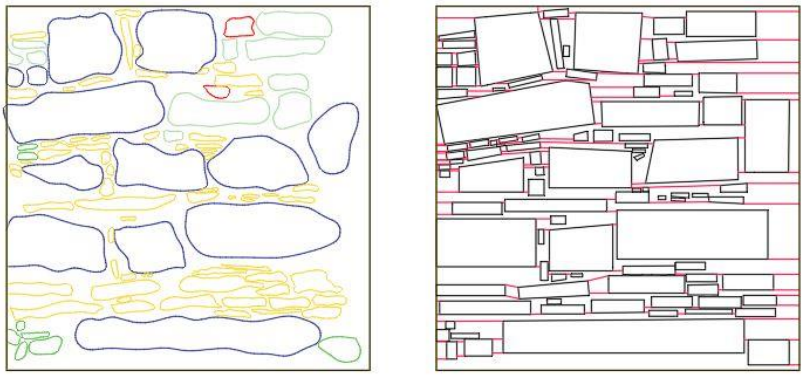

Figure 5.6. Longitudinal Wall

The valuable information about the structural behaviour can be obtained from the data collected during the analysis at the monitoring points. The first monitoring point was chosen near the line where the prescribed displacements were applied. The second monitoring point was chosen at the support, in order to obtain the value of reaction. The disadvantage of ATENA 2D is that it can not provide a summation of reactions, so they were obtained from output reports and summed manually in Excel. The strain of the model was calculated as the total displacement divided by the length of the model, while the stress in the wall was obtained as the sum of all reactions divided by the width of the wall. Load-displacement curves can be seen in Figures 5.7 and 5.8.

In Appendix B is possible to observe the propagation of cracks, as well as the distribution of stresses.

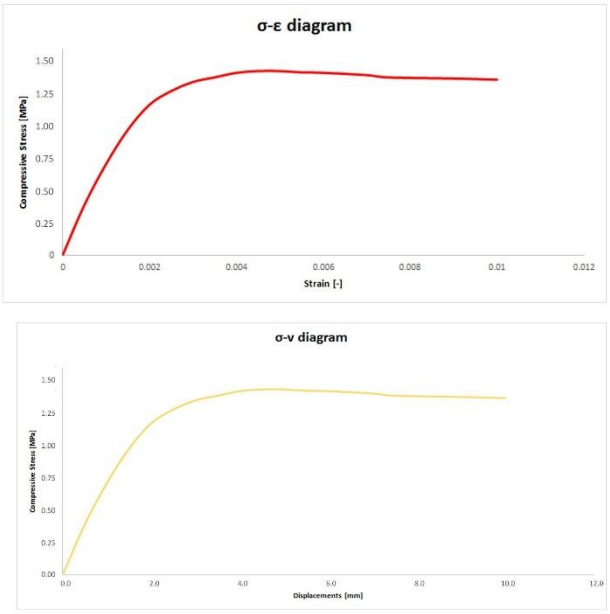


Figure 5.7. Results for Facade Wall

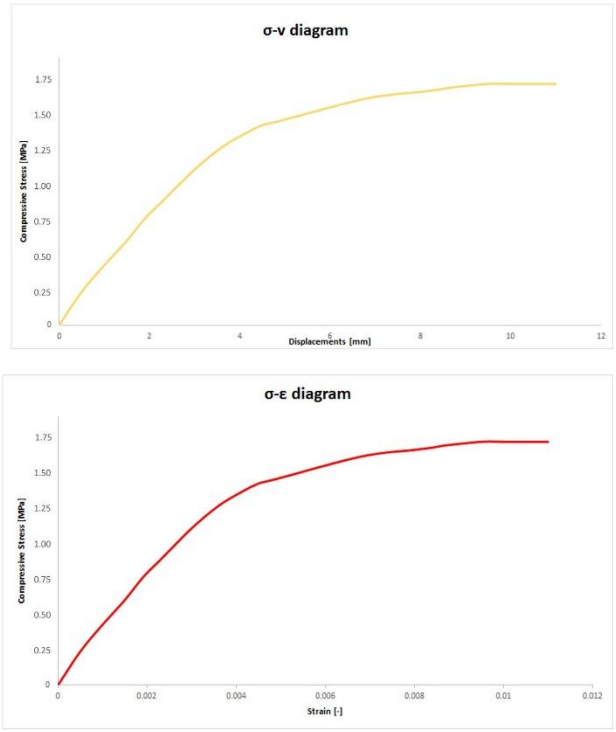


Figure 5.8. Results for Longitudinal Wall

Acquired results from ATENA 2D software for peak compressive strength of the masonry longitudinal wall and estimated values of tensile strength and Young's modulus can be observed in Table 5.3.

Table 5.3. Obtained results for longitudinal Walls

| Longitudinal Wall | Peak compressive stress [Mpa] | Estimated Tensile Strength [MPa] | Young's Modulus [GPa] |
|---|---|---|---|
| Facade | 1.45 | 0.145 | 1.26 |
| Longitudinal | 1.70 | 0.17 | 1.05 |

## 5.7 Sectional Wall

Additionally, finite element analysis was done for transversal or sectional walls. Usually, existing masonry walls are made of multiple leaves, which was also the case in St Barbara Church. Three-leaf wall, with external leaves made of sound stones and the width of 0.5m and middle between them is filled with rubble, with a width of 0.4m. Due to the lack of the available tests to examine the middle leaf, two different models were assumed in order to present sectional walls accurately. The main difference in distinct modeling approaches was the existence of a connection between the leaves (stones that go through the width of the wall and connects external leaves). In the case of multi-leaves walls, with poor

interlocking, the separation can occur, which can lead to buckling of individual parts and out-of-plane failure.

Stress-displacement and stress-strain diagrams for the can be seen in the following Figures 5.9 and 5.10.

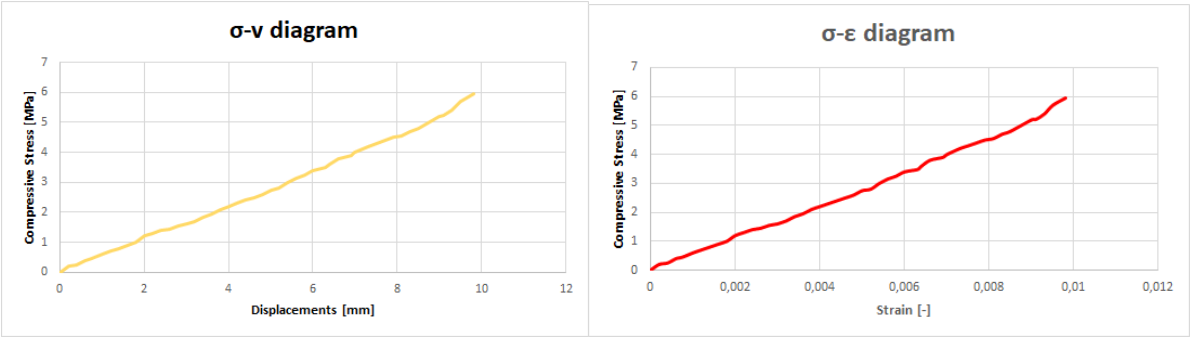


Figure 5.9. Sectional wall with interlocking stones

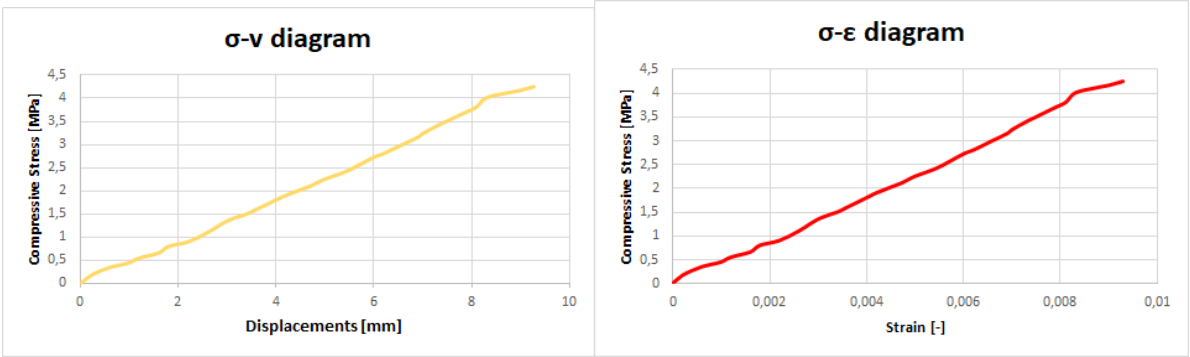


Figure 5.10. Sectional wall without interlocking stones

Obtained results for maximum compressive strength, as well as estimated values for tensile strength and Young's modulus, can be seen in the following Table 5.4. Higher values are, logically, acquired for the wall with interlocking stones.

Table 5.4. Obtained results for Sectional Walls

| Sectional Wall | Peak compressive stress [Mpa] | Estimated Tensile Strength [MPa] | Young's Modulus [GPa] |
|---|---|---|---|
| With interlocking stones | 5.95 | 0.6 | 0.58 |
| Without interlocking stones | 4.24 | 0.45 | 0.47 |

## 5.8 Current Loading Situation

After the nonlinear analysis and obtaining the σ-ε diagram, values of maximum compressive strength in the wall should be compared with the level of current stresses present in the wall.

*Self Weight of Masonry*

The density of masonry was taken as 20 kN/m3. The acting area is thick 1.4m and high 15.5m. The linear load is equal to 434 kN/m.

*Self Weight of Timber roof*

Due to the lack of information about roof truss of the St Barbara Church, data for St Jacob Church, from the thesis of Giulia Facelli [5], was used, since geometry, engineer and method of the building are very similar.

Total self-weight consists of the weight of the roof cover, main truss, beams supporting the platform and beams supporting the ceiling. The load coming from the roof cover is equal to 0.93 kN/m2, and the weight of the beams supporting the ceiling is 0.5 kN/m2. The linear load distributed on the walls is taken as 25 kN/m.

*Live Load*

According to Eurocode 1, roofs that are not accessible except for maintenance and repair should be designed with a live load of 0.4 kN/m2. Although, according to Table A1.1of Eurocode 0, along with snow, the combination factor is taken as 0.

*Snow Load*

According to the National Annex of the Czech Republic, characteristic snow load ($s_k$) that should be considered in the Broumov region is equal to 2.25 kN/m2.

Roughly calculated compressive stress at the base is 0.34 MPa.

The calculated value is much smaller than the compressive strength of the wall that was obtained previously by FEM modeling. This means that the walls do not have issues with load-bearing capacity and that the damages observed on site are due to the other causes.

# 6. SOIL-STRUCTURE INTERACTION

When dealing with historical constructions, it is highly important to know about foundations, since differential settlements could be the reason for crack development and different damages.

Soil is a heterogeneous material consisting of a solid skeleton of grains in contact with voids filled with gas, water or other fluid [13]. It transmits compression and shear stresses. When subjected to the load, soil changes its material properties [14]

Ground deformation is one of the major causes of damage in the structures. Modeling of soil presents a very demanding task due to its heterogeneity.

Analysis of soil became possible with the improvement of the finite element method, as well as analysis of soil/structure interaction. Depending on a distance from the loading point, soil can work in the elastic or plastic range. Therefore, in numerical computations, it is fundamental to define the behaviour of soil through its constitutive model.

## 6.1 Soil-Structure Interaction

It is very difficult to characterize soil accurately due to its high heterogeneity which originates in a mixture of solid fraction, water and air. Usually, in engineering practice, modeling of soil is simplified, and foundations are represented as a point, line or area support, free or fixed. This approach is valid for the structures with deep and stiff foundations, but historical buildings usually do not comply with this assumption. Their foundations are often more flexible and very shallow, due to the limitations in a process of construction and the load-bearing walls are very thick. Also, this assumption should not be used in case of less stiff soil. Moreover, differential settlements can cause multiple issues (cracking, instability) in a structure, and this phenomenon must be treated correctly.

In general, two methods can be used to model structure-soil interaction (Breeveld). One is modeling the structure as a beam/plate element resting on the elastic subsoil layer, while the other is the continuum approach using finite element analysis. Both methods consider the deformation of soil and structure.

One of the possibilities for the first method is Winkler (one parameter) model and is simpler to use. This method approximates the subsoil as a set of vertical springs. It is based on the proportion between the compression stress and vertical displacement at each point of the contact area.

$$q = k \cdot w$$

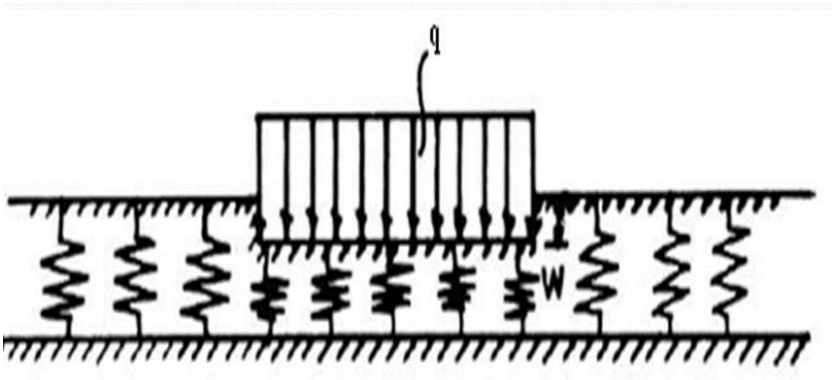


Figure 6.1. Winkler model [15]

K is defined as a modulus of subgrade reaction or the subsoil stiffness. It depends on the loads, shape and dimension of foundations.

The limitation of the Winkler model is that it does not consider the interaction between springs, so each spring behaves independently, and it does not take friction into account in the contact area, making it not very realistic.

Further research in this field had a goal to include the effect of shear (Grasshoff, Heteny, Vlasov, Pasternak). Subsequently, Pasternak suggested model which connects the springs by introducing a thin elastic membrane at the top, subjected to the constant horizontal tension. His model can take into account the actual shearing effect of soils in the vertical direction. This approach yields more accurate results than Winkler.

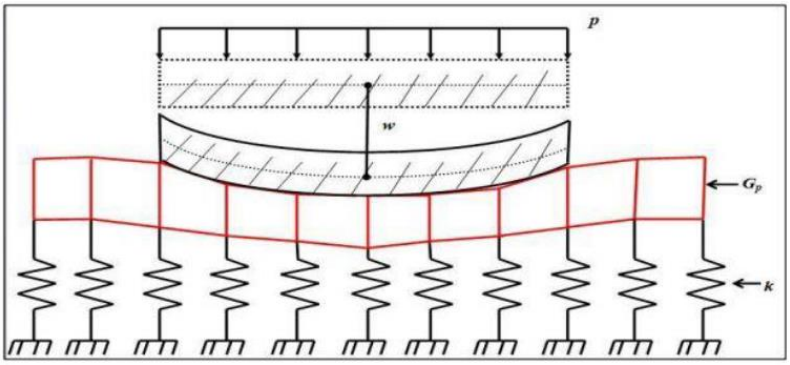


Figure 6.2. Pasternak model (Breeveld)

Also, two parameters need to be defined. The commonly used formula is

$$c_1 w - c_2 \Delta w = f_z$$

which is an equilibrium equation in the vertical direction. Constants $c_1$ and $c_2$ represent compressive and shear deformability. The author of this model suggested plate loading tests to evaluate these two parameters.

The main advantage of the Pasternak model, apart from taking into account the reduction effects of the shear stiffness of soils on differential displacements, is that it can take into consideration surface displacements outside the beam to a greater degree than the Winkler model (T. Hideaki).
Depth software obtains equivalent constants for a single elastic layer of soil for a set width and load [16]. The constants from Depth program will be used in the 3D model of the Church, to estimate a spring constant.

The second method of the modeling of soil is the continuum approach, where the layers of soil are assumed as continuously distributed matter through space. The simplest constitutive model to represent soil is linear elastic isotropic. Analysis of the continuum model can be carried out with the Finite Element Method (FEM) and with BEM (Boundary Element Method). In the case of the nonlinear constitutive model of soil, FEM is a better solution, while in the case of semi-infinite linear elastic analysis, BEM might be a better choice.
One of the most famous theorems for the analytical solution for the continuum approach is the Boussinesq theory. His formula is based on the assumption that soil is semi-infinite, homogeneous and isotropic, that it has a linear stress-strain relationship, that soil is weightless and the load is a point load acting on the surface. The following formula is derived for infinite strip loads regardless of Poisson's ratio.

$$\sigma_z = \frac{3Q}{2\pi z^2}\frac{1}{\left(1+\left(\frac{r}{z}\right)^2\right)^{\frac{5}{2}}} = \frac{Q}{z^2}I_B$$

Parameter $I_B$ is the Boussinesq coefficient, z is the vertical distance (depth) between the point where the load is applied and the point for which the stress is calculated, while r is horizontal distance between the same points.

## 6.2 Depth of Influence Zone

In order to calculate the deformation of the elastic layer in the vertical direction, the depth of an influence zone is fundamental. Horizontal displacements are neglected, resulting in a stiffer soil response. Additionally, soil "remembers" the highest level of loading that it was subjected to, which is mathematically represented by the over-consolidation ratio. Before the first loading, in its virgin state, the deformability of soil is very high (Kuklik, 2010). The concept of the influence zone can be explained by using the following Figure 6.3:

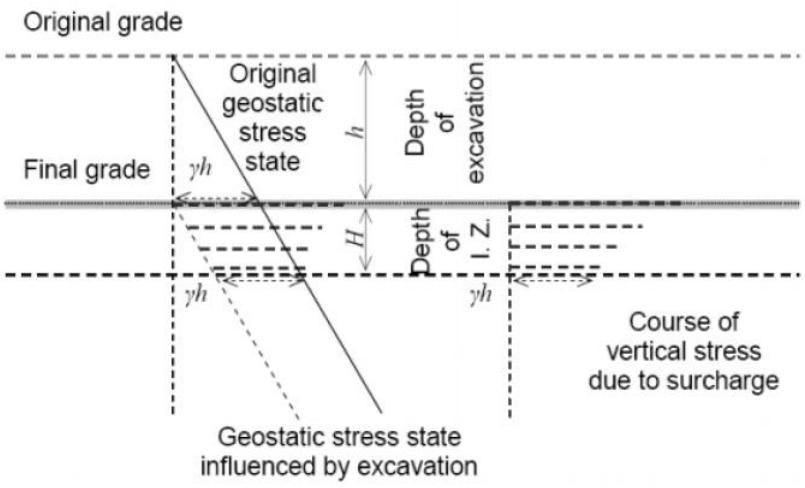


Figure 6.3. Depth of Influence Zone (Kuklik, 2010)

The original geostatic stress state is defined by the initial compaction of soil represented by the preconsolidation pressure. After excavation (depth h), the highest stress level in the prior loading history is reduced. Additional load at the bottom of footing causes the redistribution of the vertical stress. If the vertical effective stress, due to this additional load, in combination with the reduced geostatic effective stress, due to the excavation, does not exceed the original geostatic effective stress, the deformations are negligible and this zone is considered as the influence zone (Kuklik,2010). A formula that provides a good estimation of the depth of the influence zone due to the uniform load strip fz with a width of 2a can be noticed below.

$$H = \frac{\pi a}{2}\left(\frac{2-2\upsilon}{1-2\upsilon}\right)^{\frac{1}{2}} \frac{1}{\ln\left(sin\frac{\pi\gamma h}{2f_z}+1\right)-\ln\left(\cos\frac{\pi\gamma h}{2f_z}\right)}$$

It is important to notice that the influence zone does not depend on Young's modulus, but it does on the Poisson ratio.

As it was already mentioned, Software Depth will be used for the calculation of the depth of the influence zone.

## 6.3 2D Model

Simplified 2D model of the church is made in FINE GEO5 software, in order to estimate the effect of soil settlements on the structural behaviour of the Church. Although it is a 2D model, it can be beneficial as a preliminary model and provide an idea about settlements. Software FINE GEO5 uses a continuum soil approach.

### 6.3.1 Modeling Assumptions for GEO5 Analysis

The analysis done in software GEO5 is based on the hypothesis of plain strain. Thus, only the transversal sections of the wall along with the different layers of soil were modeled. Boreholes test provided enough knowledge to characterize different layers and to assign them different mechanical properties. The wall was modeled with a thickness of 1.4m, which corresponds to the real width of the three-leaf wall, while the height of the wall is 15.5m. In GEO5 software it is possible to define different stages of the construction process in order to see the change in settlements due to additional weight. Due to the simplicity of the model, roof loads were taken into account through an increase in density of the walls, from 20 kN/m3 to 22 kN/m3. [10]

Regarding the constitutive model of soil, in software, it is possible to analyze a purely isotropic material, which is not very accurate. The more realistic assumption would be modified elastic law, which assumes different material response in loading and unloading. For this model, it is necessary to know $E_{ur}$, which is unloading-reloading Young's modulus.

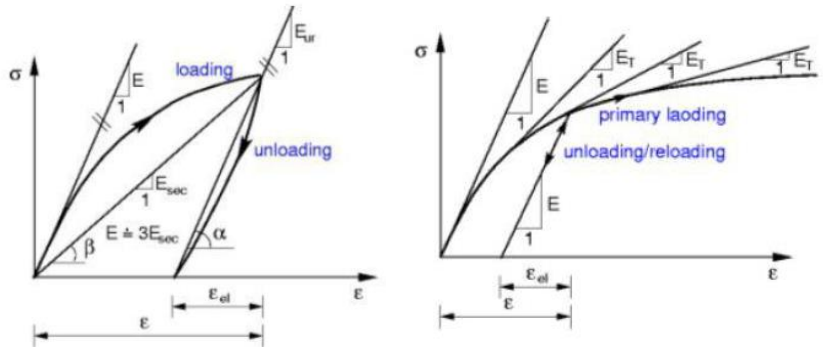


Figure 6.4. Real behaviour of soil (left) and Mohr-Coulomb model (right)

For this analysis, the Mohr-Coulomb failure criterion is used. This nonlinear law unites three concepts, plain strain transformation equations, Mohr's circle, and Coulomb's failure criterion. Coulomb's criterion requires two material parameters in order to describe the failure in the soil - the angle of friction $\varphi$ and the cohesion c. Mohr-Coulomb's model gives accurate results for the materials whose compressive strength exceeds the tensile.

In Otavice, where St Barbara church is located, the bedrock consists mostly of siltstones, sandstones, and claystones. These stones are classified as sedimentary, as they were formed in the process of sedimentation, which is accumulation or deposition of small mineral or organic particles on the seabed. The surface layer is composed of sandy soil with a small amount of claystone. The colour of layers changes from red-brown to gray claystone in the bottom. Compaction and degradation due to the weathering are different for each layer. The geological map of Otovice can be seen in Figure 6.5.


Figure 6.5. Geological Map of Otovice (366- gray sandstone, 360- siltstone, 2053 - limestone.) (Geology.cz)

The footing masonry is made of natural stone, very similar to the underlying rock. The reason behind it is that ancient masons were using material from the nearby surrounding. Due to weathering, building stones lose the original properties, which usually results in a decrease of compressive strength or durability. The underlying rock also changes mechanical characteristics, for instance, cohesion. Water has also a significant role in the mechanical behaviour of stone. Durability is directly conditioned by the presence of water. In the liquid state, water dissolves chemical compounds and can lead to the crystallization of salts. Furthermore, ice and salt crystallization may cause high pressures, which usually surpasses the tensile strength of the stone. The presence of water can also cause dissolution and leaching of binder which negatively influences the cohesion.

The clastic sedimentary stones are the most sensitive to weathering. The reason is the arrangement of its internal structure, especially the abundant presence of interconnected pores. Therefore, it is of the highest importance to eliminate the water income into the footing masonry and underlying rock.

The soil under the Church seems to be uniform, which results in the low possibility for differential settlements. If the condition of stone material gets worse, the stability of the whole structure might be threatened, thus monitoring of foundations and soil is recommended (Kovářová,2019).

Layers of the soil under the Church and pictures of boreholes can be found in Appendix C. Since several layers have similar mechanical properties, four were grouped in macro groups, as can be seen in Table 6.1

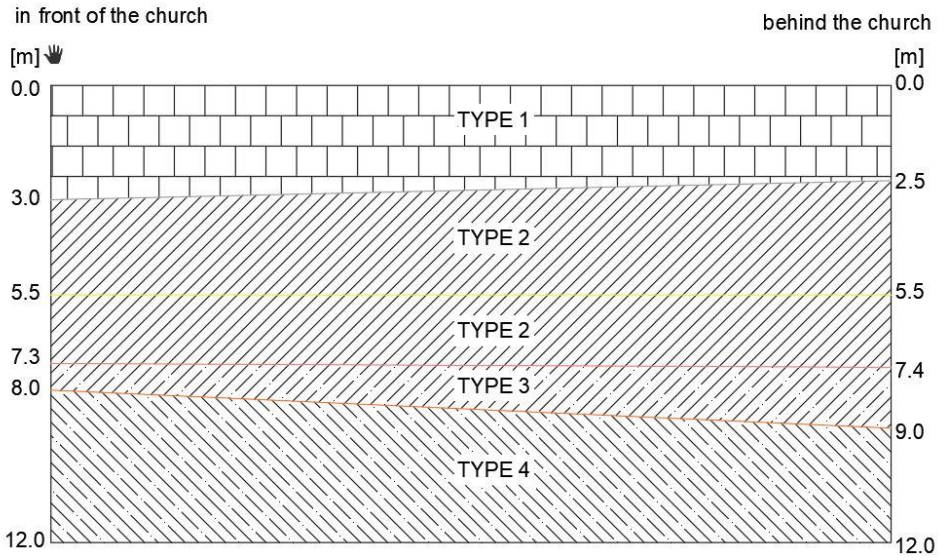


Figure 6.6. Layers of soil

Table 6.1. Mechanical properties of different layers of soil

| Soil Type | Edef [MPa] | $\nu$[-] | $\varphi$[○] | c`[kPa] | $\gamma$[kN/m3] |
|---|---|---|---|---|---|
| Type 1 | 20 | 0.35 | 25 | 30 | 19.5 |
| Type 2 | 25 | 0.35 | 30 | 30 | 20 |
| Type 3 | 30 | 0.35 | 30 | 40 | 20.5 |
| Type 4 | 30 | 0.35 | 30 | 50 | 20.5 |

Building a model in GEO5 software was carried out in multiple stages, in order to simulate the process of construction of the Church. Only sectional walls were modeled, as plain strain assumption was made. The first stage presented the virgin state of the soil, second stage the excavation up to the depth of the foundations, and third, fourth and fifth stages simulated construction of a wall. The total height of the wall is 15.5 m

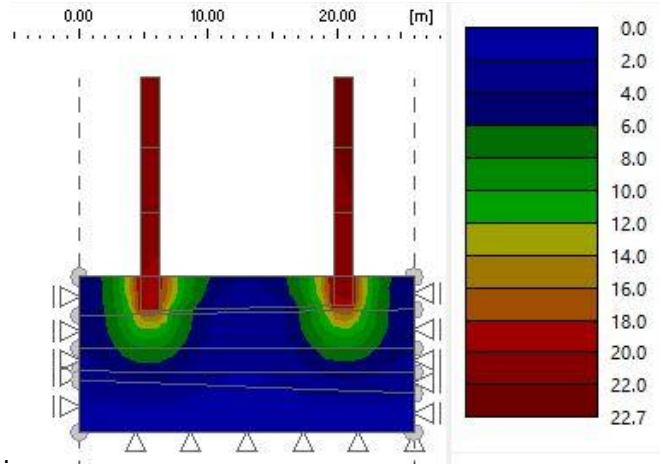


Figure 6.7. Stage 5 - Displacements [mm]

In Appendix C, different phases of construction can be seen with diagrams of vertical stresses and vertical displacements.

Maximum displacement due to the self-weight and roof loads is reached in the final stage and is 22.7 mm.

## 6.4 Conversion of Subsoil Properties into Spring Constants

In order to have more realistic supports, and thus, the more realistic results, the springs were applied to the bottom of the foundations. It was assumed that springs are elastic and it was necessary to calculate their stiffness. The deformation modulus k can be calculated as [16]

$$k = 2\sqrt{c_1 c_2} + c_1 b$$

First, it is needed to obtain Winkler Pasternak constants, $c_1$ and $c_2$. This can be done by using software DEPTH, as it was already mentioned. In DEPTH, it is possible to take into account only one layer of soil, so the equivalent values of parameters are required. The equivalent Young's modulus is calculated as 25.07 MPa and the equivalent Poisson's ratio is 0.3. Surcharge applied is 480.81 kN/m, which came from self-weight of the wall and the roof truss.

Computed values of $c_1$ and $c_2$ are 9.825 MN/m$^3$ and 5.403 MN/m, respectively, as it can be observed in Figure 6.8

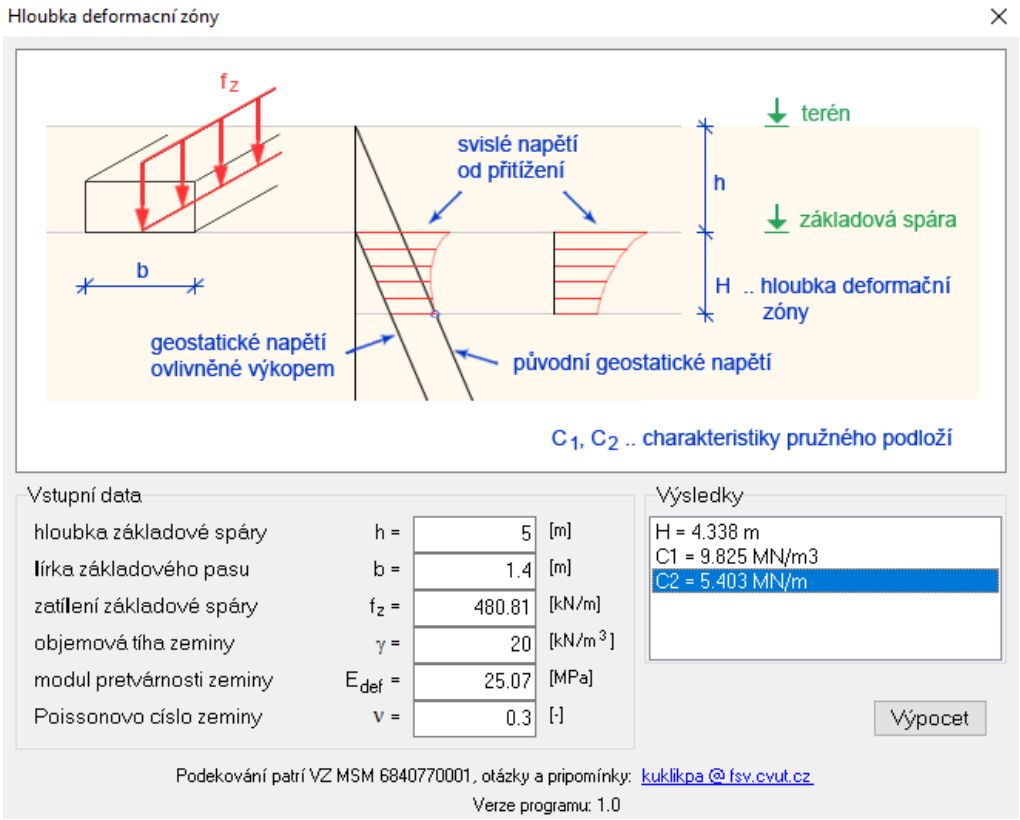


Figure 6.8. Calculation from software DEPTH

Analytical solution of Winkler Pasternak equation is given below:

$$f_z = w_s(2\sqrt{c_{1w}c_{2w}} + c_{1w}b)$$

where $f_z$ (kN/m) represents the total load acting on subsoil, $c_{1w}$ and $c_{2w}$ are Winkler Pasternak constants, and b (m) is the width of the foundation, while $w_s$ is displacement.

The modulus of deformation was calculated and is 26.36 MPa,as it can be found in Table 6.2. below.

Table 6.2. Values of influence zone depth, constants and deformation modulus for springs

| Eeq [MPa] | H [m] | C1 [MN/m3] | C2 [MN/m] | k [MPa] |
|---|---|---|---|---|
| 25.07 | 4.338 | 9.825 | 5.403 | 26.36 |

## 6.5 Conclusions on settlements

In order to define the maximum admissible values of the crack width of heritage masonry structures, it is important to take into consideration the historic value of the construction, structural role of an element that is cracking and the exposure class of material.

# 7. 3D ANALYSIS

In most engineering applications, masonry is assumed as a continuous and homogeneous material for modeling purposes (Lourenço and Pereira 2018). This strategy is the most appropriate for large-scale models and allows optimization of time and storage requirements to develop the model (implementation of the geometry and generation of the mesh) while providing adequate results for the analyses (Lourenço 1996).

The 3D analysis of the Church aims to investigate its structural behaviour more accurately, by using the finite element method. FEM software that was used is ATENA 3D Science, which allowed running nonlinear analysis and application of different plasticity models.

## 7.1 3D Model

After obtaining accurate dimensions of the Church on site, it was possible to build a 3D model that represents well the actual geometry. Minimal simplifications were done, in order to avoid mesh issues. Also, decorative parts were not modeled, due to their insignificant influence on structural behaviour. A very complex timber roof was not investigated in detail in this thesis, but it is assumed that the thrust from the roof applied to the robust masonry enclosure walls is negligible. This is the reason why the roof was not modeled, but its self-weight, live and snow load were applied as a vertical load on the top of the enclosure walls.

The foundations of the church are relatively shallow, with a depth of 2.5m in front of the Church and 3m at the back.

At the bottom of the foundations, elastic springs were modeled in order to better simulate the soil under the Church. In the previous chapter, the deformation modulus *k* was obtained, and the value of the initial stiffness of spring was calculated by dividing *k* with the thickness of the wall (1.4m).

Linear tetrahedral elements were chosen for modeling. Mesh size used was 0.01 in order to ensure a good compromise between accuracy and computational cost.

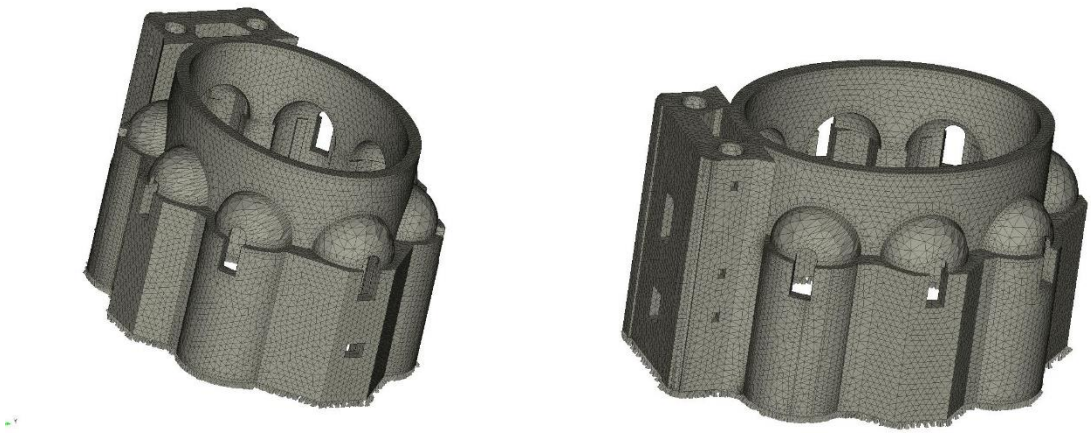

Figure 7.1. 3D model of the Church

## 7.2 Material Properties

The nonlinear cementitious model was chosen and that is a fracture-plastic model that combines constitutive models for tensile and compressive behaviour. [11]
This model is based on the orthotropic smeared crack formulation. It incorporates Rankine failure criterion, exponential softening and it can be used as a rotated or fixed crack model. Rankine failure criterion assumes that if the maximum tensile strength is reached in any direction, the material will break. Softening can be explained as a gradual decrease in mechanical resistance under the increase of deformation.[12]
Crack concepts can be divided into discrete concepts and smeared concepts. In smeared concept, a crack is still a continuum. Smeared crack concepts can be classified as fixed and rotating smeared crack concepts. With a fixed concept the orientation of the crack is the same during the entire computational process, whereas in rotating, the orientation of the crack to co-rotate with the axes of principal strain.

The rotating model was used for the 3D model of the Church, since the information on shear strength and shear retention factor are not known, and the rotating model was found as a more accurate solution. Cracking is quantified by the integral of the stress-strain diagram, denoted as fracture energy $g_f$ for tension and $g_c$ for compression. [17]

First, it was necessary to decide which material properties to assign to the model.
After performing the analysis on the part of the wall (Chapter 5), the value of compressive strength was obtained. Also, these values were compared to the values in the Italian Code [18]. The values of the other parameters were later calculated, for instance tensile strength as a 1/10 of the compressive strength. The relation for obtaining Young's modulus of masonry is $E=\alpha f_c$, with values of $\alpha$ varying between 200 and 1000 (Tomazevic, 1999).

| Masonry typology | Compression strength $f_m$ (MPa) min–max | Shear strength $\tau_o$ (MPa) min–max | Young modulus E (MPa) min–max | Shear modulus G (MPa) min–max | Weight density W (kN/m$^3$) |
|---|---|---|---|---|---|
| Irregular stone masonry (pebbles, erratic, irregular stones) | 1.0<br>1.8 | 0.020<br>0.032 | 690<br>1,050 | 230<br>350 | 19 |
| Uncut stone masonry with facing walls of limited thickness and infill core | 2.0<br>3.0 | 0.035<br>0.051 | 1,020<br>1440 | 340<br>480 | 20 |
| Cut stone with good bonding | 2.6<br>3.8 | 0.056<br>0.074 | 1500<br>1,980 | 500<br>660 | 21 |
| Soft stone masonry (tuff, limestone, etc.) | 1.4<br>2.4 | 0.028<br>0.042 | 900<br>1,260 | 300<br>420 | 16 |
| Dressed rectangular (ashlar) stone masonry | 6.0<br>8.0 | 0.090<br>0.120 | 2400<br>3,200 | 780<br>940 | 22 |
| Solid brick masonry with lime mortar | 2.4<br>4.0 | 0.060<br>0.090 | 1,200<br>1,800 | 400<br>600 | 18 |

Borri et al. (2015)

Figure 7.2. Estimated values for different masonry [18]

Selected values can be seen in the following Table 7.1.

Table 7.1. Chosen values for 3D model

| E [GPa] | v | fc [MPa] | Gc[N/m] | ft [MPa] | Gt [N/m] | ρ [kN/m3] |
|---|---|---|---|---|---|---|
| 1.3 | 0.2 | 3.0 | 7200 | 0.3 | 50 | 20.0 |

## 7.3 Elastic Analysis

The elastic analysis was carried out in order to verify the model and to compare the settlements obtained from GEO5 Analysis. Under foundations, a set of springs was applied with the stiffness of 26.36 MPa. Applied loads were the self-weight of the structure and roof load applied on the top of the enclosure walls. The highest value of displacement was obtained as 18 mm. GEO5 analysis provided results of 22.7 mm, validating both analyses.

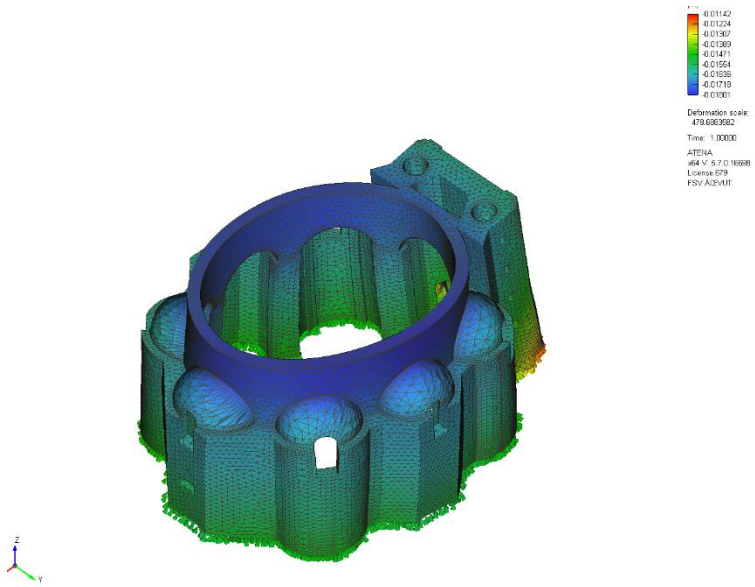

Figure 7.3. Displacements

## 7.4 Nonlinear Analysis

The nonlinear analysis was carried out in order to determine the reason why some cracks appeared, to verify if it is due to differential settlement and to obtain the knowledge about the overall behaviour of a structure due to the latter.
Although the cracks are not very common, as it was observed during in situ inspection, the aim of this analysis was also to check under which load structure would start having stability issues.

As it was already mentioned, the soil around and under the Church seems to be in a very good condition, showing only slight deterioration in the areas close to the gutters. Due to the water flow, the soil is eroded, and this could be a possible reason for settlement and cracks in the walls. Few hypotheses will be verified, depending on the location of the gutter and the level of decay of soil.

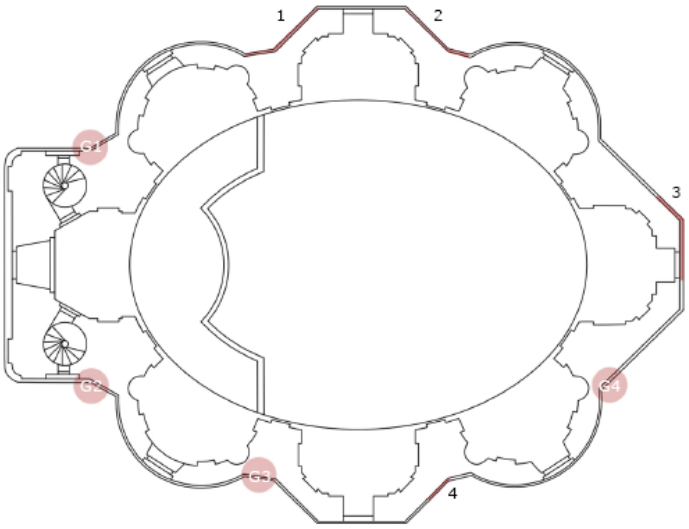


Figure 7.4. Location of gutters and settlements

In Figure 7.4, map with the location of gutters and settlements cracks can be seen. The effects of deteriorated soils were modeled not only through the springs with the low stiffness, but also as prescribed vertical displacement.

Imposed displacements were applied in regions that are prone to settling, in multiple steps, in order to get the propagation of the cracks and evolution of the stresses. The bottom of the foundations was divided into the zones, in order to allow easier settings of displacement.

## 7.5 Settlements in Area S1

The first hypothesis assumed the vertical settlement under the part of the longitudinal wall, as it was shown on a map.

In the area S2, an imposed settlement of 5cm in 20 steps was applied. Some of the steps (5,10,15,20) are shown in Figures 7.5 and 7.6. Crack propagation can be seen here, and stress distribution can be found in the Appendix D. The maximum crack width at the basis is around 3 cm, which might have resulted due to the concentration of stresses, so more spread value of crack width is 1.8cm.

After five steps, the magnitude of settlements was 1.25 cm, and at that moment, crack width was close to 1 cm, imposing that even low level of settlements could cause moderate damage.

It is important to understand the propagation of cracks, as its aspect should be monitored in the future. Cracks above the windows, in the arches, could be explained through this assumption.

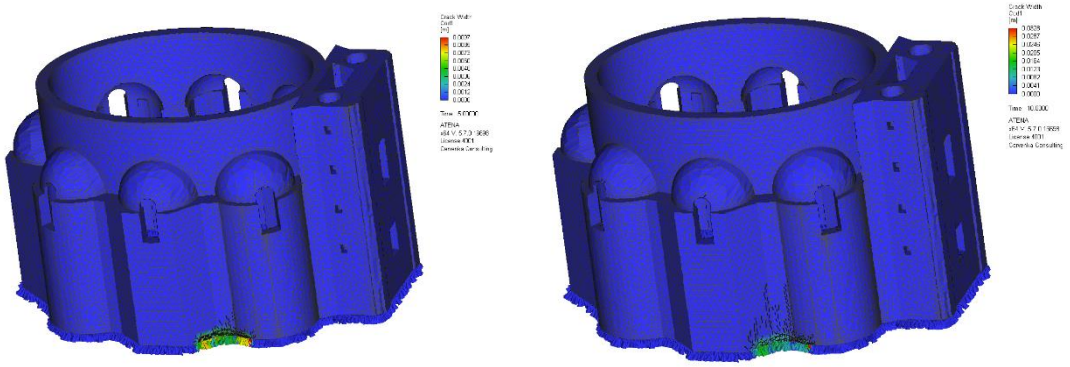

Figure 7.5. Load step 5 (left) and load step 10 (right)

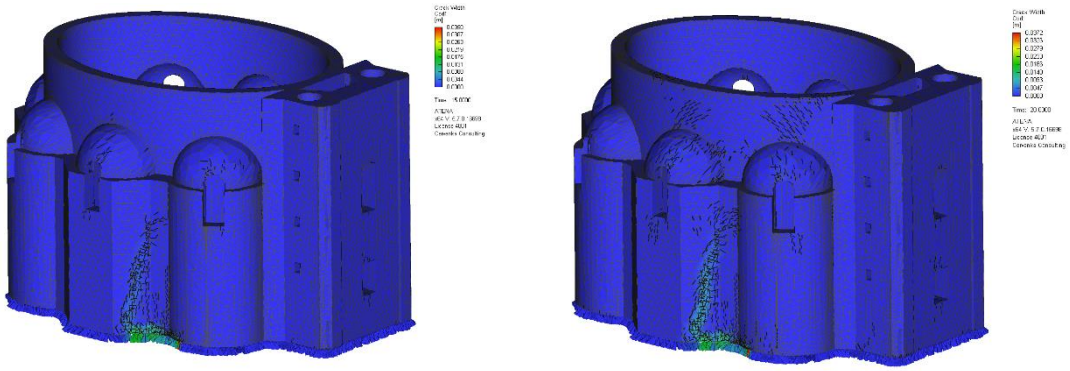

Figure 7.6. Load step 15 (left) and load step 20 (right)

## 7.6 Settlements in Area S2

The settlement was applied in the area S2, diagonally from the location of the second assumption. Imposed settlement of 3 cm was applied in 15 steps. Crack propagation and opening of cracks can be seen in the following Figures_.

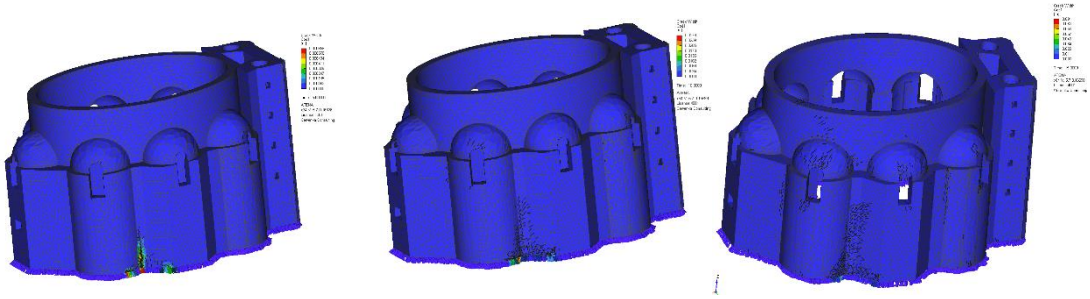

Figure 7.7. Step 5 (left), Step 10 (middle) and Step 15 (right)

Differential settlement in this area of 3 cm, causes the maximum width of a crack less than 1 cm.

## 7.7 Settlements in Area S3

Area S3 is located at the back of the church, under the chancel. Visual inspection indicated that few stones are misplaced, with cracks between blocks. Behaviour due to two different load cases were checked, one with an imposed displacement of 3 cm applied in 10 steps, and the other with a displacement of 5 cm in 20 steps. In the following Figures 7.8, 7.9, 7.10, stress state as well as crack propagation can be found.

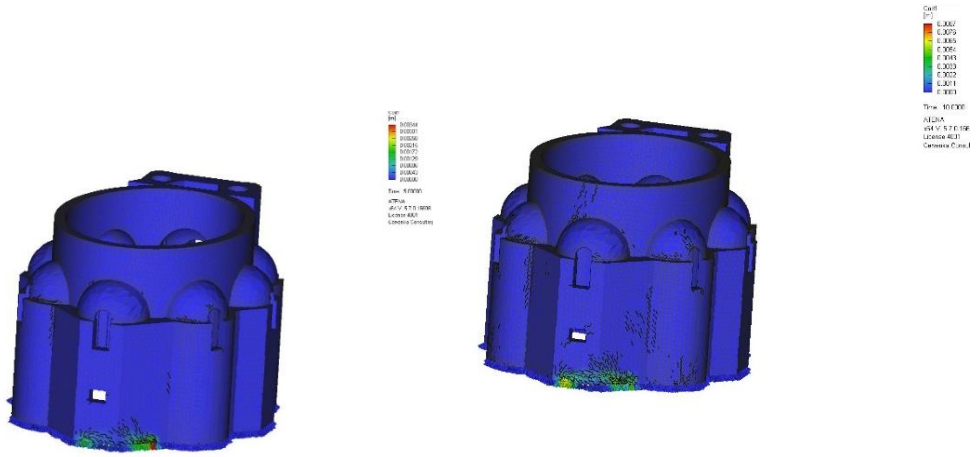

Figure 7.8. Step 5 (left) and step 10 (right) – analysis with a settlement of 3 cm

Analysis with 3cm of imposed displacement gave the maximum crack width of 7mm. As this assumption did not meet reality, another analysis with a prescribed displacement of 5 cm in the same area was carried out.

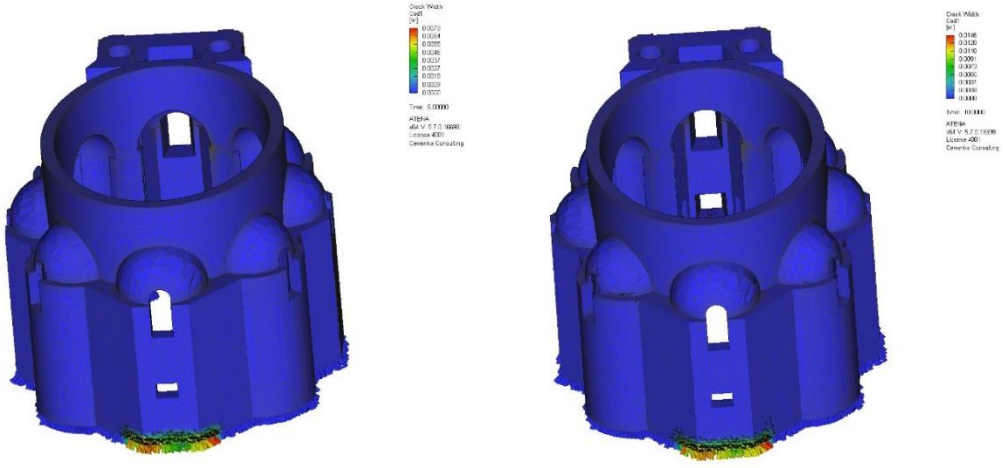

Figure 7.9. Step 5 (left) and Step 10 (right) - Analysis with settlement of 5 cm

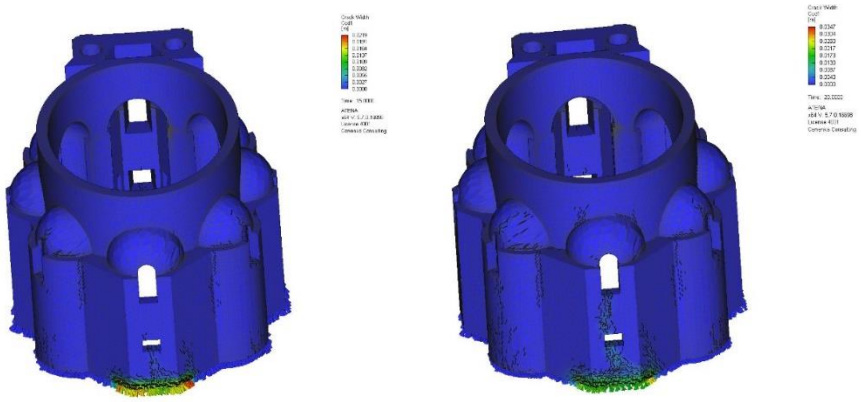

Figure 7.10. Step 15 (left) and Step 20 (right) - Analysis with settlement of 5 cm

In step 20, the width of the cracks is around 2.5 cm, at the base of the wall. In step 15(3.75 cm applied) , the crack width is around 2 cm, in the 10th step (2.5cm) crack width is around 1cm.

## 7.8 Conclusions on Settlements

As it was already mentioned, cracks due to differential settlements do not seem to be very common in St Barbara Church. After nonlinear analysis, it was understood that settlement around 4-5 cm would cause an opening of cracks wide 2-2.5 cm, which would possibly cause the issues. Moreover, the analysis confirmed the good condition and stability of the Church. In any case, the monitoring system which would control displacements and cracks opening should be installed in the Church.

Table 7.2 (Burland, 1977), gives a threshold of crack width related to the severity of the damage. From the analysis, it is clear that the severe or very severe damage would occur only if the crack width is higher than 1.5 cm, which would occur in St Barbara Church after the differential settlement of more than 2.5cm. At this moment, it does not seem probable that differential settlement occurs in this magnitude.

However, the appearance of the crack above the window (mentioned in Chapter 4), could have happened due to differential settlements in Areas 2 or 3. The crack pattern observed on-site coincides with one provided by ATENA software, meaning that one of the first locations where cracks would occur is in the arch above the window. Diagrams aquired from 3D Analysis could be found in Appendix D.

Table 7.2. Degree of damage regarding crack width

| Degree of damage | Description of typical damage | Approximate crack width |
|---|---|---|
| (0) Negligible | Hairline cracks. | < 0.10 mm to 0.15 mm |
| (1) Very slight | Fine cracks which can easily be treated during normal conservation/decoration works. | ~ 1 mm |
| (2) Slight | Cracks which can be easily filled and probably require re-decoration. Possible need of repointing to ensure weather-tightness. | < 5 mm |
| (3) Moderate | Moderate cracks which can be easily patched or masked by suitable linings. | 5 mm to 15 mm |
| (4) Severe | Large cracks which require extensive repair work. Impair of functionality. | 15 mm to 25 mm |
| (5) Very severe | Very large cracks which require major repair job. Danger of instability. | > 25 mm |

# 8. CONCLUSIONS AND RECOMMENDATIONS

The case study was performed on St Barbara Church in Otovice, the Czech Republic in order to analyze load-bearing capacity of the enclosure walls and overall stability of the Church. The conclusions obtained will be presented in this Chapter.

The first part of the thesis was focused on the cultural importance of the Church, as well as its history and reasons why it is necessary to protect built heritage in the Broumov region. After that, visual inspection and damage mapping were carried out, and the general idea of the good condition of the Church was formed. Compared to the other Broumov churches, St Barbara is in a much better state, probably due to a new drainage system, which keeps the water far from the structure. Deterioration of render was present all over the facade, but it does not seem to cause any further problems to the structural behaviour of the church. Cracks were found only on few spots, and their cause was explained by the settlement of the soil.

The main part of the thesis was concentrated on the calculation of bearing capacity of the robust masonry walls, which was achieved by the means of 2D micro modeling of part of the wall. Values of compressive strength (3 MPa), tensile strength (0.3 MPa), Young's modulus (1.3 GPa) were obtained by combining the results from 2D analysis and recommendations from Italian code [18].

The current level of stress due to self-weight and roof and live loads seems to be 10 times lower than the maximum compressive strength of the masonry walls, confirming the hypothesis of a low level of damage in the structure and good overall condition.

The uniform settlement was calculated by using GEO5 software and ATENA, obtaining results around 2 cm of vertical displacement.

Finally, as cracks are not very common in the Structure, nonlinear analysis with soil settlements served more as a reference if future settlements would lead to more severe damage. Furthermore, horizontal cracks could occur due to the change of water content in the soil, especially in freeze-thaw cycles, but right now there is no sign of this type of damage.

To conclude, from a structural point of view, the enclosure walls do not show any problems that would affect the stability of the Church. However, more information on the condition of foundations and soil, as well as properties of materials should be collected.

**Recommendations**

As the Church is in good shape, all the recommendations here proposed are based on the further nondestructive or minor destructive tests and analysis, in order to acquire more accurate data and reduce the number of uncertainties. Moreover, previous interventions should be identified and controlled through these tests. Noninvasive tests and sustainable and compatible interventions are fundamental, due to the historical importance of the Church.

Geometry

Since historical masonry buildings work usually only in compression, their functionality is based on the geometry. Regarding the geometry of the Church, it is necessary to perform a more thorough survey, which would provide knowledge of the thickness of all the elements, especially ones with limited access. Since masonry structures are often inhomogeneous and full of irregularities, the wall thickness may not be constant, internal voids should be discovered and the presence of multiple leaves and their connection should be checked. Boroscope could be a cheap solution, while impact echo test could discover the shape of interlocking stones.

Materials

Quality of materials and level of deterioration can vary throughout the Church. Electromagnetic methods (radar) can be used to discover if the moisture and salt are present in walls and to determine their level. More accurate values of mechanical properties may be obtained by using sonic testing, impact echo or flat jack tests. Single flat jack test allows evaluation of stress level in the wall, while the double flat jack test indicates the elastic properties of masonry.

Monitoring

It is important to monitor the propagation of the cracks in order to react on time in case of their expansion. Also, the monitoring system gives accurate and in real-time information on structural health, as well as on hidden damage mechanisms. Crackmeters could be useful for this purpose, but it is important to store data long enough to exclude the effect of the environment.

For this reason, sensors that control the humidity level and temperature should be installed in the Church.

The monitoring of soil settlements can be expensive, so it should be positioned in several places, where the soil is the most eroded (close to the gutters).

To conclude, with regular maintenance and keeping the drainage system sound, the Church will stay in good condition.

# 9. REFERENCES

[1] Internet: https://en.wikipedia.org/wiki/Bohemia

[2] Internet: https://en.wikipedia.org/wiki/Czech_Baroque_architecture

[3] Internet: https://en.wikipedia.org/wiki/Broumov

[4] Internet: https://www.broumov-mesto.cz/en/

[5] G. Facelli, “Structural survey of St. Jacob’s Church and comparison with St. Ann’s Church (Broumov group of Churches),” 2014.

[6] E. Chodějovská, E. Semotanová, and R. Šimůnek, *No Title*. 2015.

[7] Internet: https://www.broumovsko.cz/en/kostel-sv-barbory-otovice-1#prettyPhoto1/

[8] Internet: https://cs.wikipedia.org/wiki/Kostel_svat%C3%A9_Barbory_(Otovice)

[9] Internet: http://dientzenhofers.cz

[10] J. Scacco, “Nonlinear numerical evaluation of the bearing capacity and thestructure stability of the St Jacob Church from the Broumov Group of Churches”, 2018

[11] C. Republic, “ATENA Program Documentation Part 1 Theory,” 2018.

[12] P.B.Lourenco, PhD, *Computational strategies for masonry structures*, 1996.

[13] C. Aron and E. Jonas, “Structural Element Approaches for Soil-Structure Interaction,” 2012.

[14] P. Kuklik, “Fast Estimation of the Influence Zone Depth inside the Subsoil in Relation to the Various Shapes of Footing Fast Estimation of the Influence Zone Depth inside the Subsoil in Relation to the Various Shapes of Footing,” no. January, 2008.

[15] D. Crace – “Analysis of structure supported by elastic foundation”

[16] Evi Susanti – Numerical Evaluation of Bearing Capacity of the All Saint’s Church in Broumov, Czech Republic

[17] P. B. Lourenço, F. Greco, A. Barontini, and M. P. Ciocci, *Modeling of Prototype Buildings*.

[18] Circolare 617. (2009). *Circolare 617.*

# APPENDIX A – DAMAGE MAP

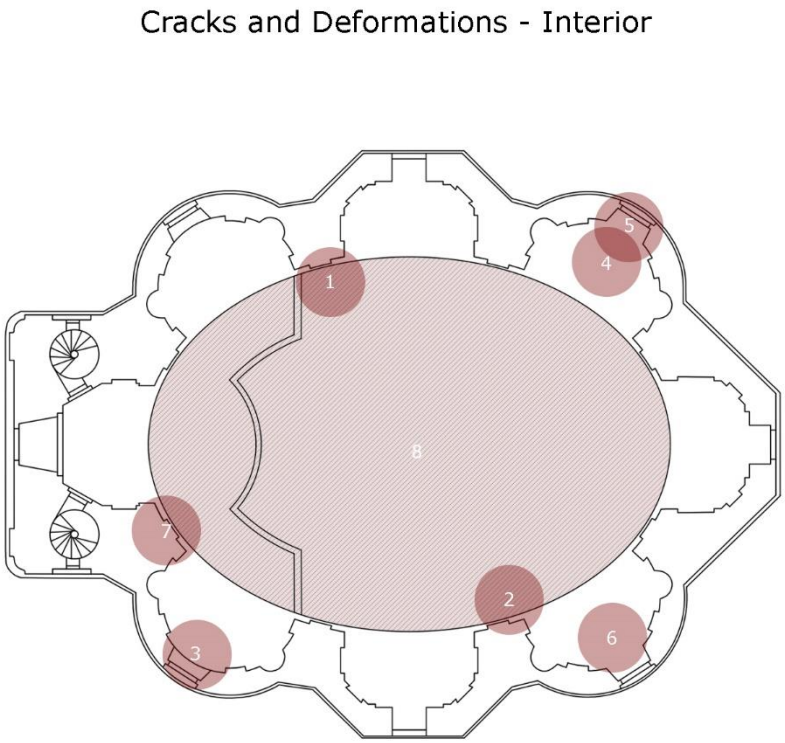


Cracks Exterior

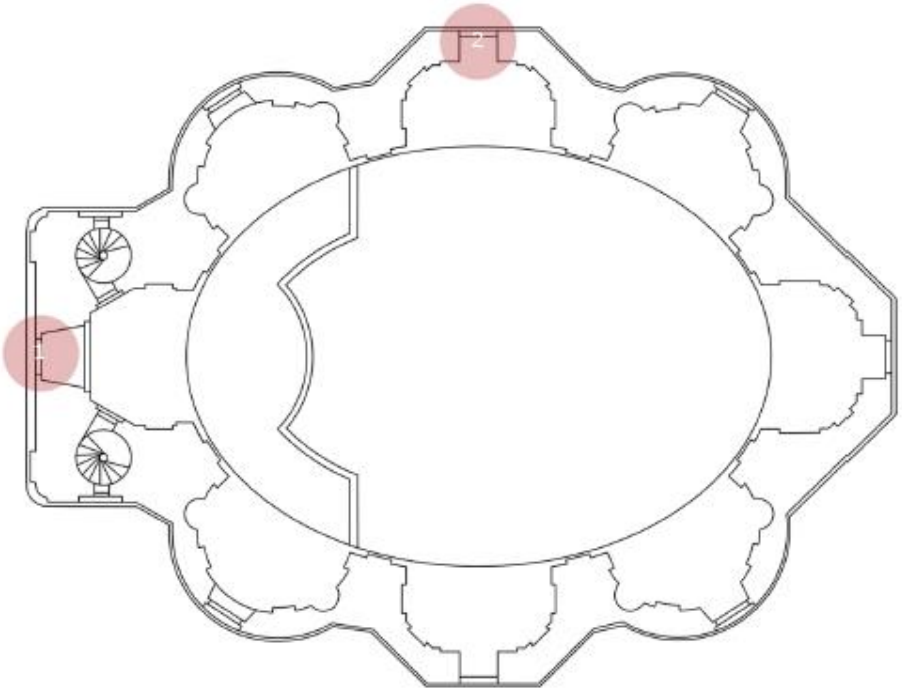


Detachments

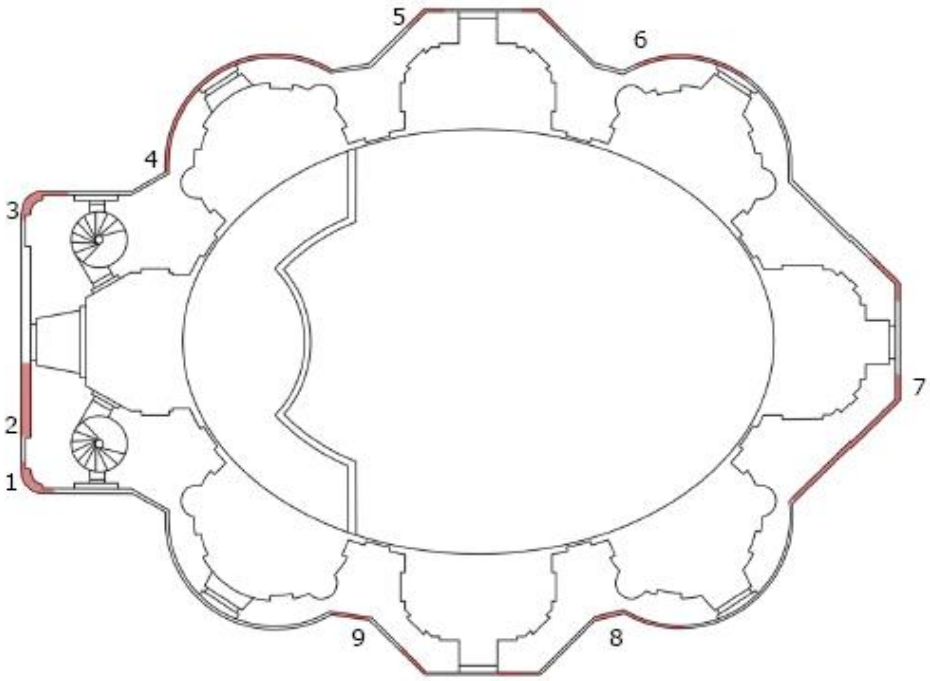


Discoloration and Deposit
**Black crust**

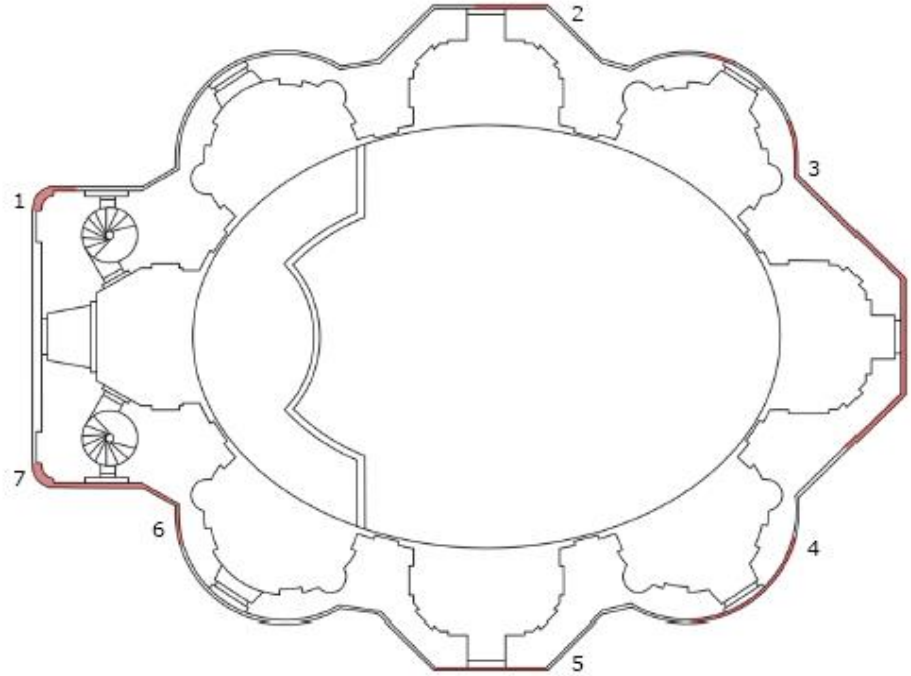


Discoloration and Deposit
**Soiling**

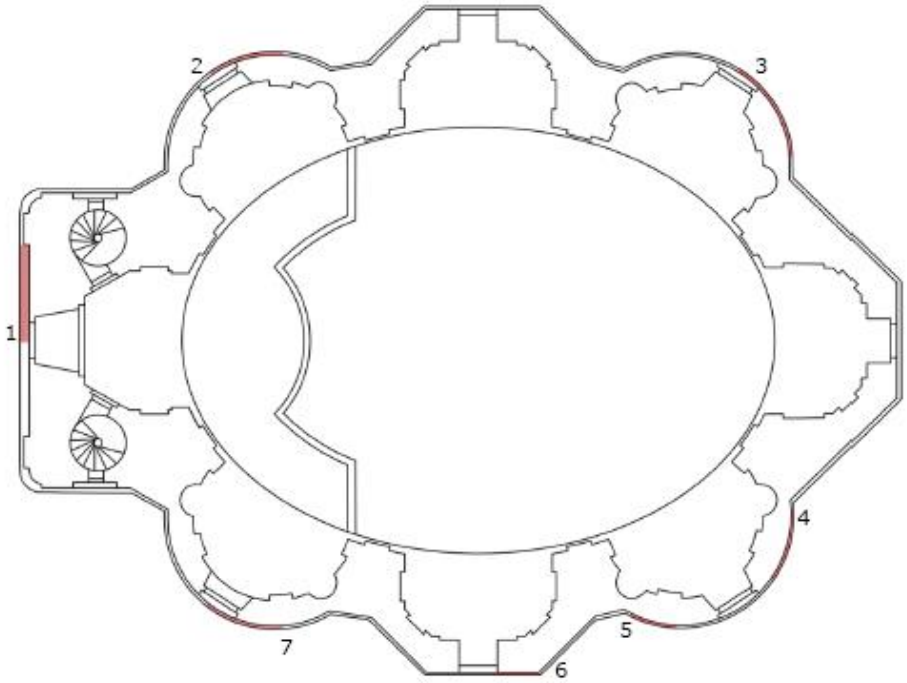


Discoloration and Deposit
**Stains**

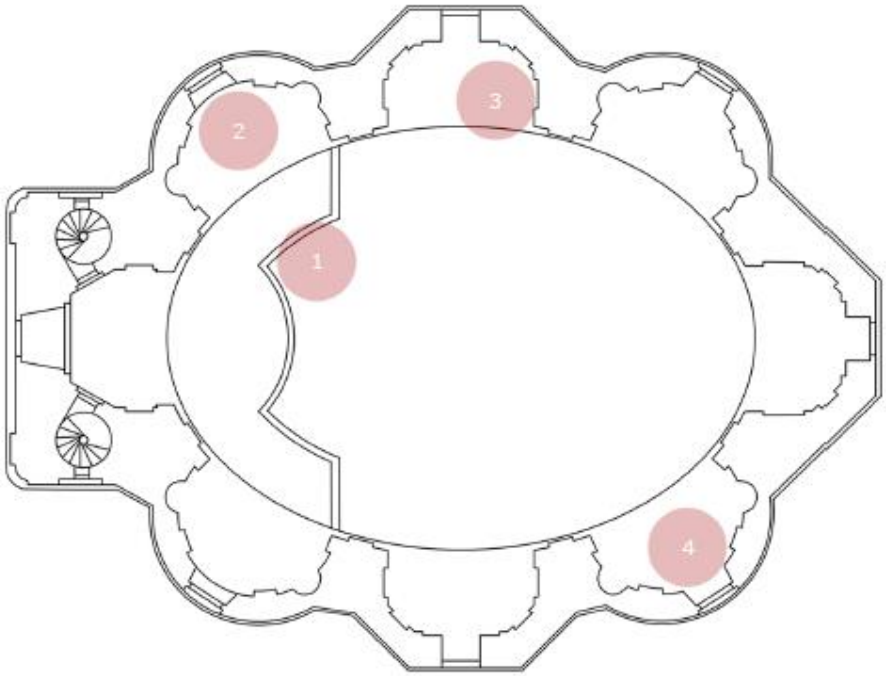


## Settlements

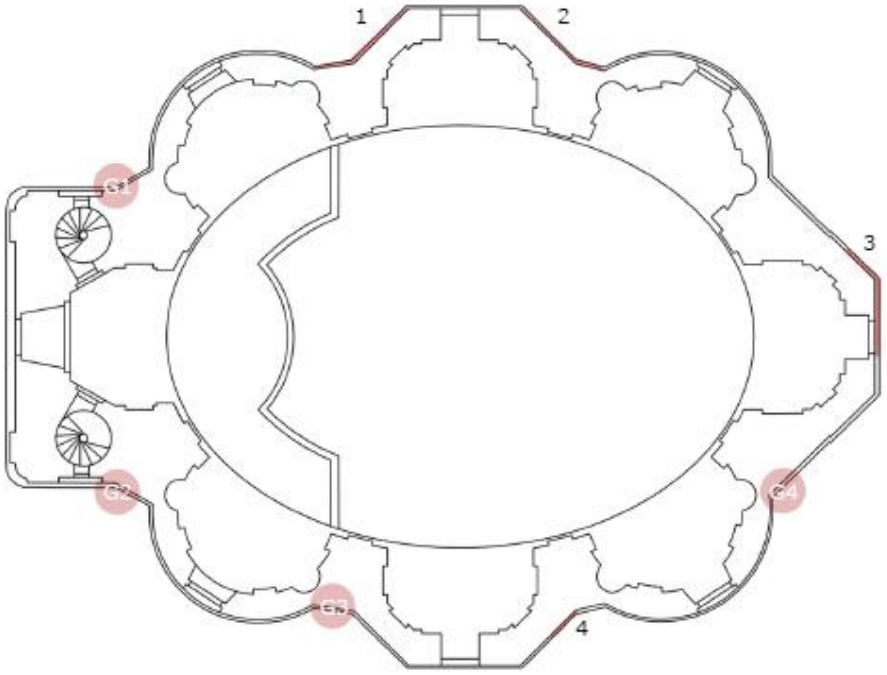


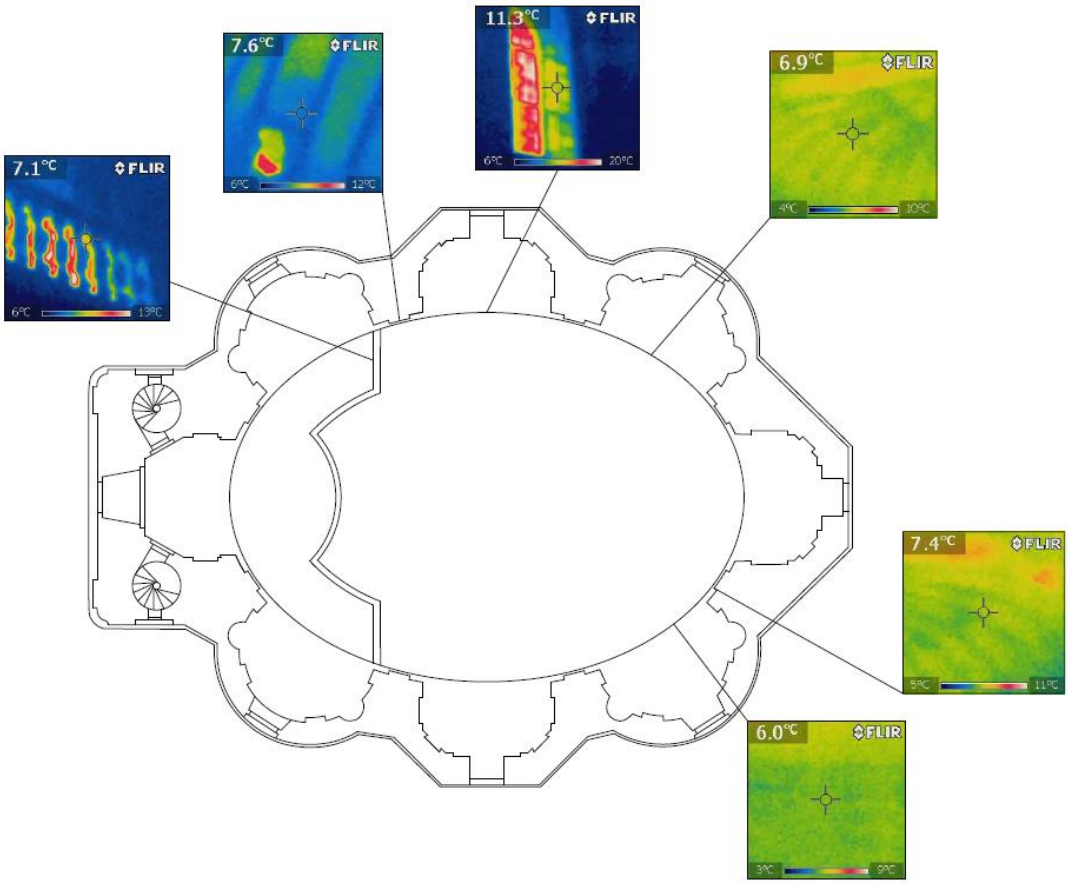


Figure 11. Thermographic Camera

# APPENDIX B – 2D ANALYSIS

- **Facade wall**

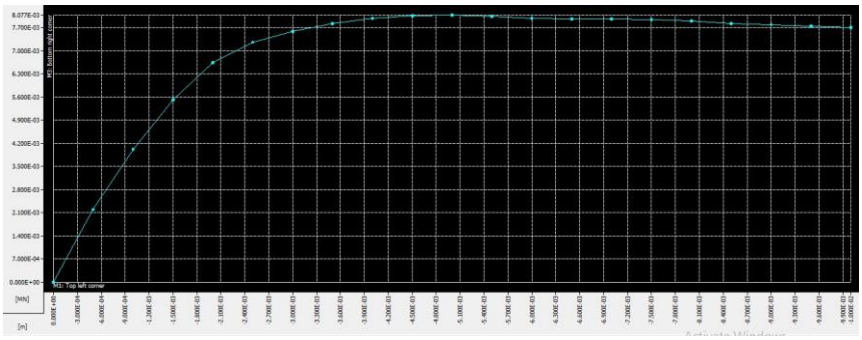

Figure 12. Diagram displacement - reaction in the step 10

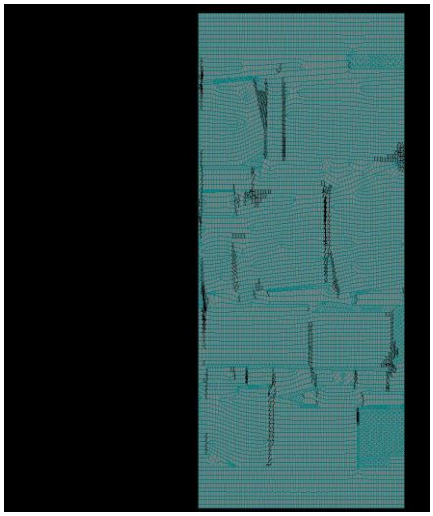

Figure 13. Step 10 - Propagation of cracks

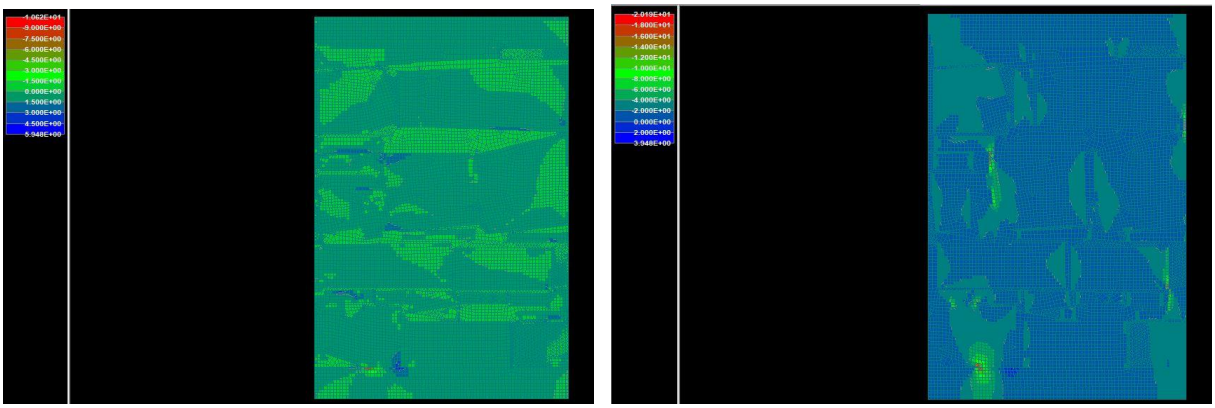

Figure 14. Step 10 - Principal stress min and max

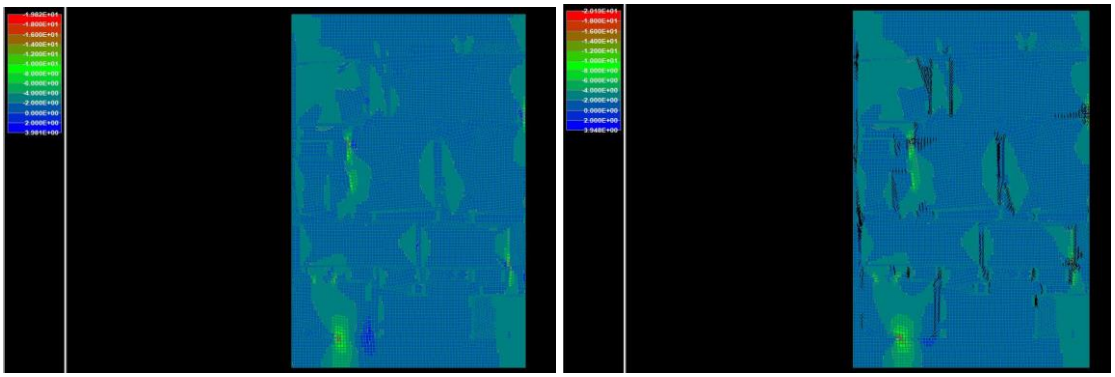

Figure 15. Stress Sigmayy and Principal Stress with Crack Propagation

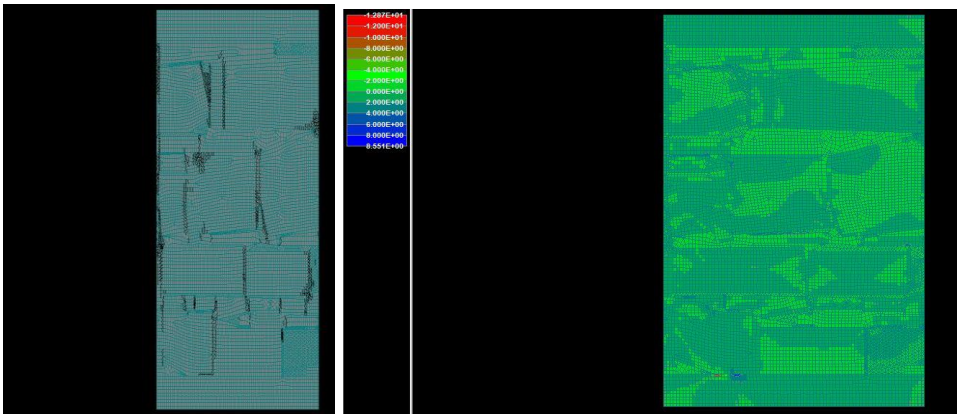

Figure 16. Step 20 (Last step) - Crack Propagation and Principal stress Max

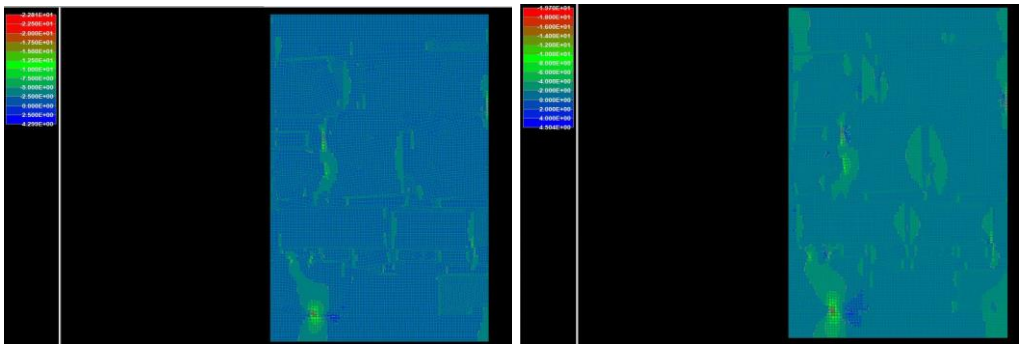

Figure 17. Step 20 (Last step) Principal Stress Min and Stress σyy

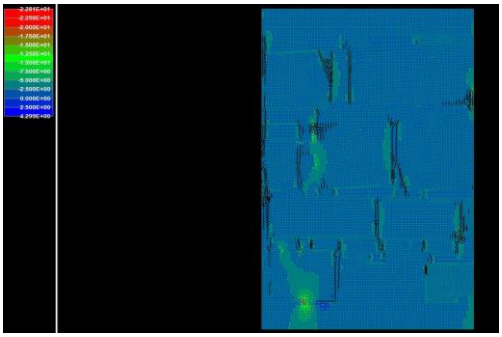

Figure 18. Step 20 (Last step) - Principal stress Min with crack propagation

- **Longitudinal Wall**

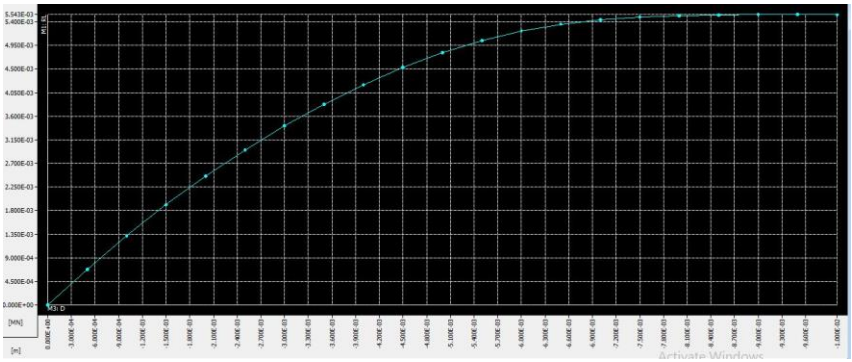

Figure 19. Diagram displacement-reaction in the step 20 (Last step)

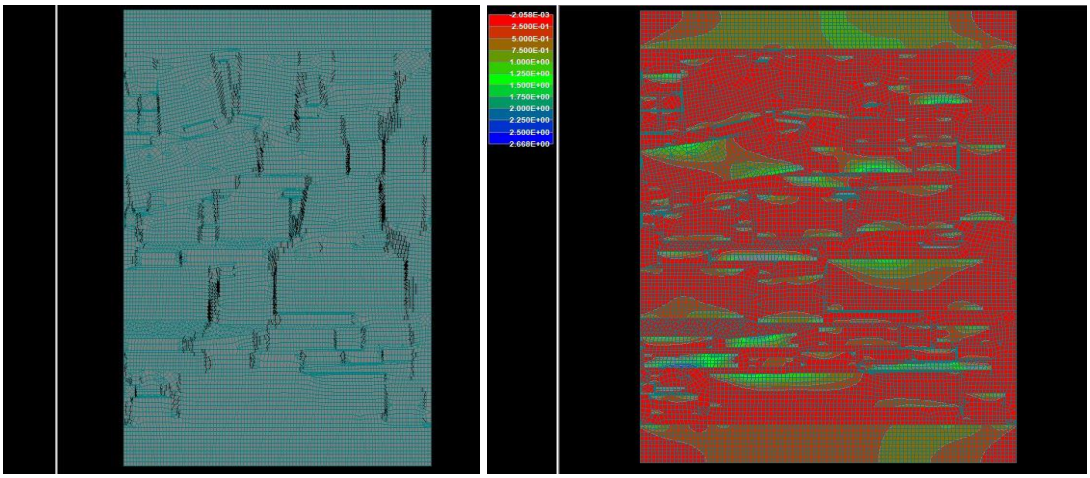

Figure 20. Step 20 - Crack Propagation and Principal stress Max

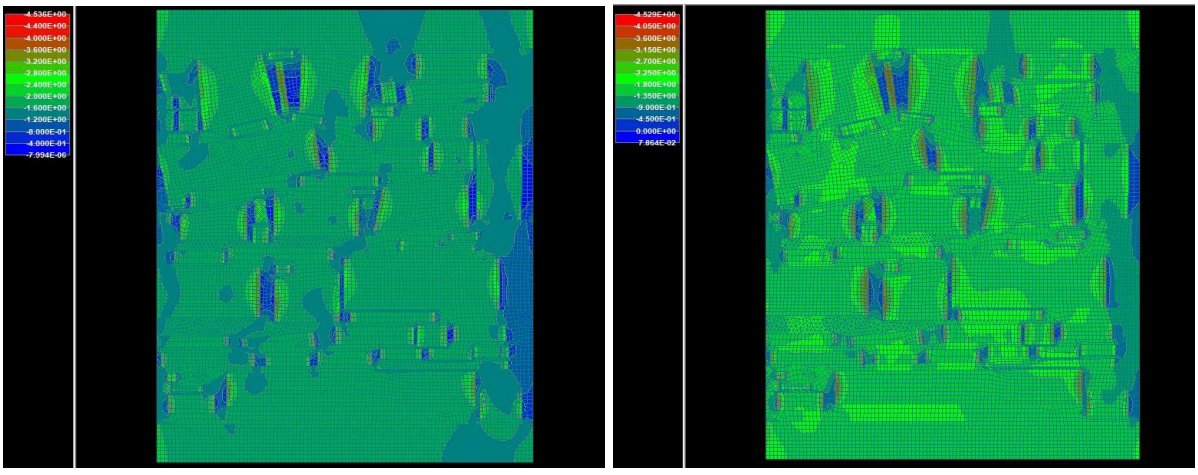

Figure 21. Step 20 - Principal Stress Min and Stress σyy

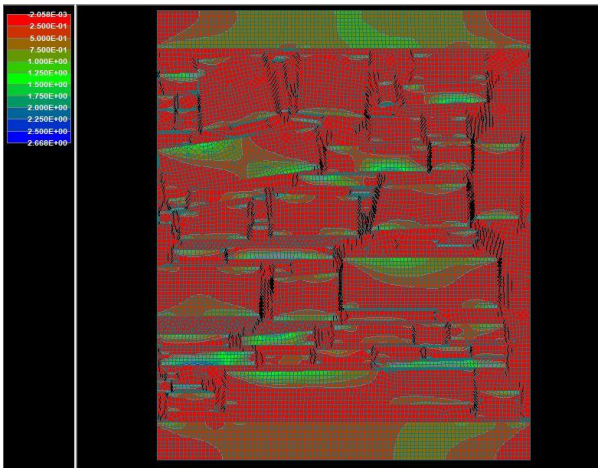


Figure 22. Step 20 - Principal stress Max with crack propagation

- **Sectional Wall with Interlocking Stones**

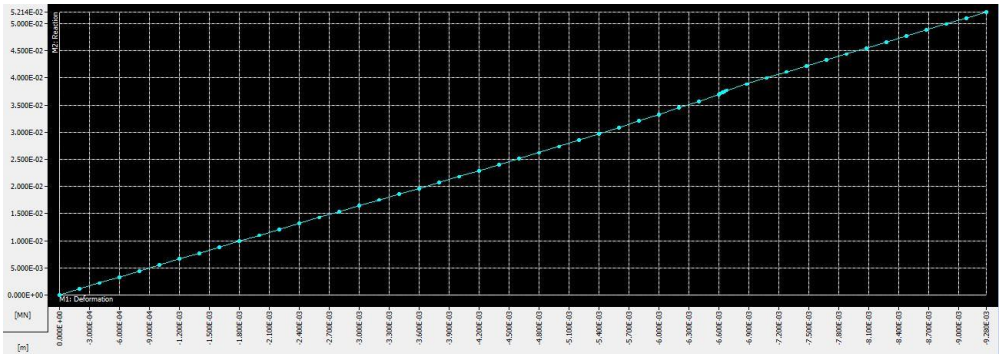


Figure 23. Step 50 - Diagram displacement-reaction

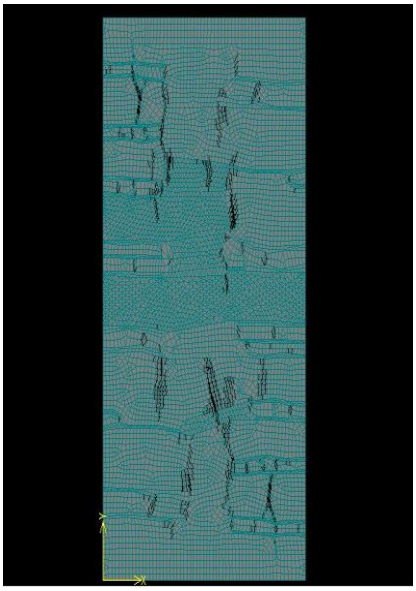

Figure 24. Step 50 - Crack propagation

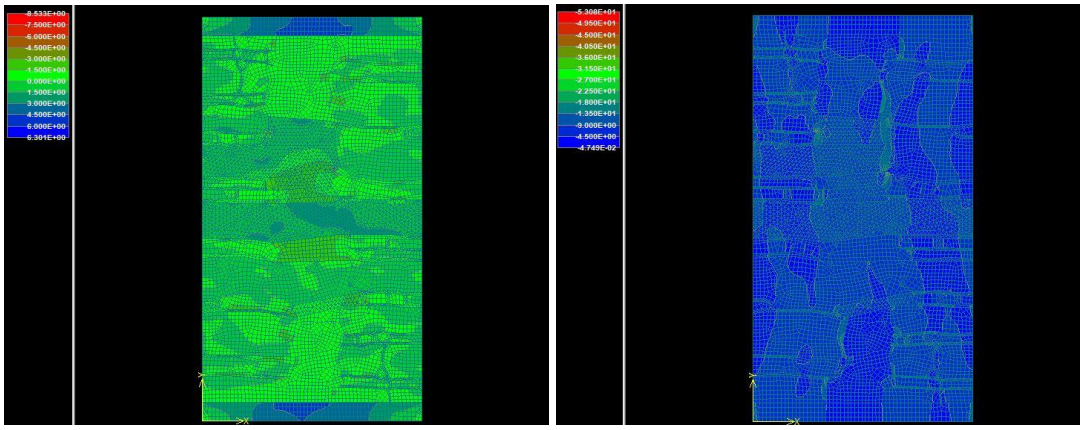

Figure 25. Step 50 - Principal stress max and min

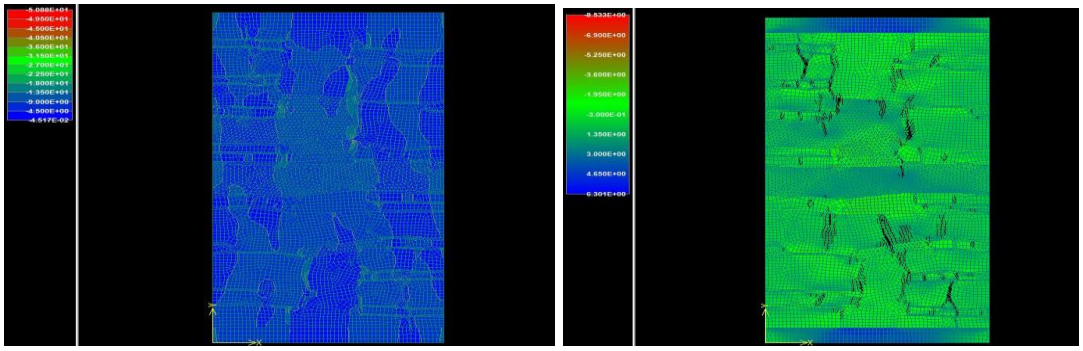

Figure 26. Step 50 - Stress Sigmayy and Principal stress Max with Crack propagation

- **Sectional Wall without Interlocking Stones**

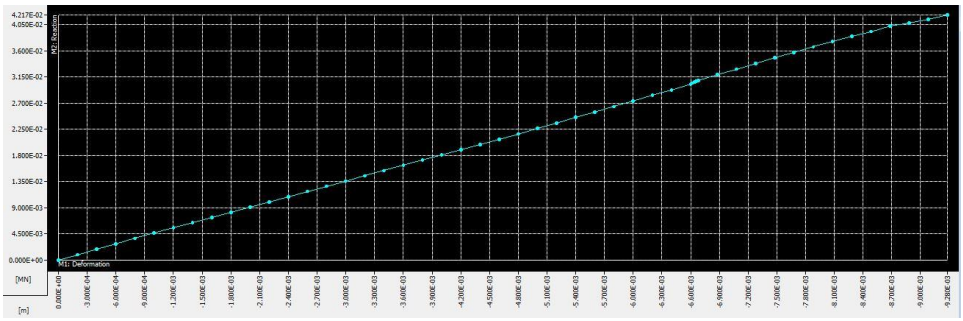


Figure 27. Step 50 - Diagram displacement-reaction

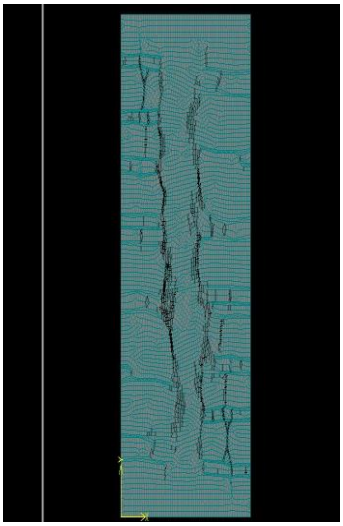

Figure 28. Step 50 - Crack propagation

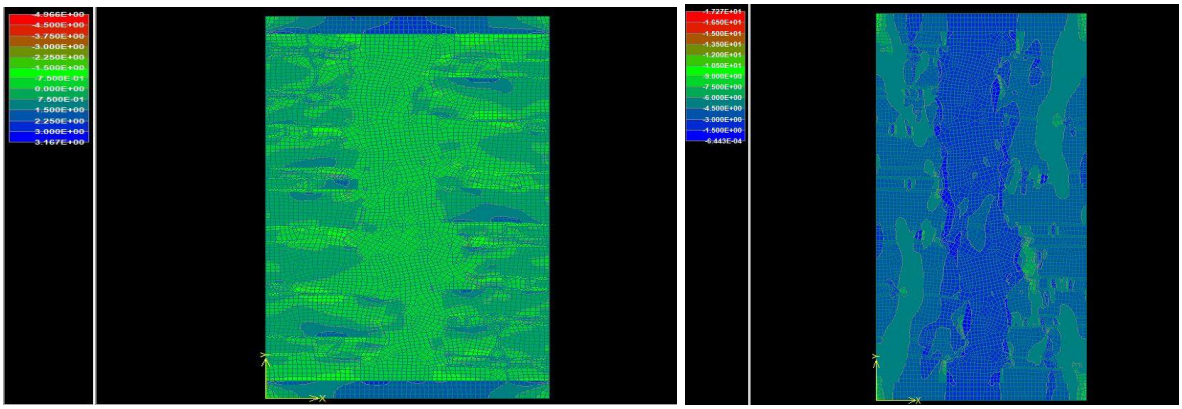

Figure 29. Figure_ - Step 50 - Principal stress max and min

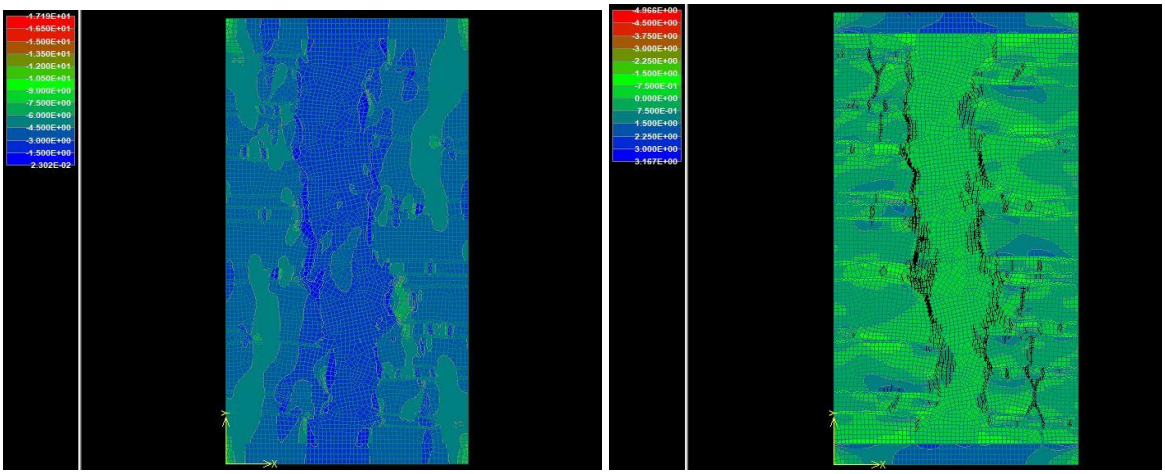

Figure 30. Step 50 - Stress σyy and Principal stress max with Crack propagation

# APPENDIX C – GEOLOGY

## Layers of soil

Table 3. Layers of soil in front of the Church

| [m] | Description |
|---|---|
| 0,0 - 1,0 | redbrown sandy soil with small stone particles |
| 1,0 - 1,2 | compact pieces of slightly weathered coarsegrained arcose sandstone |
| 1.2 | thin layer of redbrown soil with small fragments of fain grained clastic stones; easy to break down by hand |
| 1.4 | compact piece of brownreddish silty claystone |
| 1,5 - 2,0 | small pieces of brownreddish silty claystone |
| 2,0 - 2,2 | big pieces of brownreddish silty claystone |
| 2.3 | pebble of hard claystone |
| 2.4 | sandstone masonry with mortar |
| 2,4 - 2,9 | fragments of coarsegrained arcoes sandstone, easy to break down by hand; fragments of thick bedded gray claystone |
| 2,9 - 3,0 | sandstone masonry with mortar |
| 3,0 - 3,5 | small fragments of silty claystone, easy do break down by hammer |
| 3,5 - 3,7 | compact pieces of hard silty claystone |
| 3,7 - 3,9 | layer of soily character (weathered claystone) with small stone fragments |

| | |
|---|---|
| 3,9 - 4,5 | small fragmmets of silty claystone, easy to break down by hammer |
| 4.5 | compact piece of silty claystone |
| 4,6 - 5,0 | small fragments of silty claystone |
| 5,0 - 5,4 | layer of strongly weathered claystone |
| 5,4 - 5,5 | layer of strongly disintegrated to soil character |
| 5,5 - 5,6 | compact piece of silty claystone |
| 5,6 - 5,8 | small fragmmets of silty claystone, easy to break down by hammer |
| 5,8 - 6,0 | compact piece of silty claystone |
| 6,0 - 7,0 | layers of weathered finegrained sedimentary stone (claystone?), easy to break down by hammer, easy to break down by hand, in some places harder possitions |
| 7,0 - 7,3 | layer of thin bedded silty claystone, relatively hard, break down by hammer |
| 7,3 - 7,4 | layer of strongly weathered claystone |
| 7,4 - 8 | layers of weathered finegrained sedimentary stone (claystone?), easy to break down by hammer, easy to break down by hand, in some places harder possitions |
| 8,0 - 9,0 | compact pieces of silty claystone, in some places weathered layer |
| 9,0 - 10,0 | mostly weathered position, very easy to break down by hammer |
| 10,0 - 10,5 | small fragments of silty claystone |
| 10,5 - 12,0 | gray claystone, thin bedded, easy to break down by hand to thin layers |

Table 4. Layers of soil behind the Church

| [m] | Description |
|---|---|
| 0,00 - 0,30 | brown sandy soil |
| 0,3 - 0,9 | fragments of coarse grained arcose sandstone (slightly weathered), the surface is easy to crumble by hand |
| 0,9 - 1,0 | thin bedded silty claystone |
| 1,0 - 1,2 | bigger fragments of coarse grained arcose sandstone (slightly weathered), the surface is easy to crumble by hand |
| 1,2 - 1,3 | layer of strongly weathered sandstone, disintegrated to sand |
| 1,3 - 1,5 | thin bedded silty claystone to siltstone |
| 1,5 - 2 | dark redbrown sandstone, small fragments strongly weathered (extremely soft, disintegrated by hand), bigger fragments compact |
| 1.8 | claystone |
| 2,0 - 2,5 | stone fragments with mortar |
| 2.5 | big pebble of strange stone material, not weathered, hard, probably andesite (?) |
| 2,5 - 3,5 | weathered redbrown silty claystone, small fragments |
| 3,5 - 4,4 | strongly weathered layer of soil character with claystone fragments |
| 4,4 - 4,6 | redbrown claystone, easy to break down by hammer |
| 4,6 - 5,0 | compact pieces of claystones, redbrown |

| | |
|---|---|
| 5,5 - 5,5 | slightly weathered layer of redbrown claystone, easy to break down by hammer |
| 5,5 - 5,6 | layer of easy disintegrating clastic sediment of caly -silty character |
| 5,6 - 6,0 | bigger fragments of redbrown claystone, some of them easy to break down by hammer |
| 6,0 - 7,0 | sizely different fragments of easy break down redbrown claystone |
| 7,0 - 7,4 | compact and harder fragments of claystone |
| 7,4 - 7,6 | layer of brown "soil" with small fragments of fine grained sedimentary stones |
| 7,6 - 8,0 | compact fragments of claystone, redbrown, easy to break down by hammer |
| 8,0 - 8,15 | weathered greybrown classic fine grained sediment (silty claystone), easy to break down by hand to soli character |
| 8,15 - 9,0 | layer of graybrown claystone, easy to break down by hammer |
| 9,0 - 9,5 | strongly weathered claystone, disintegrated to small fragments, easy to break down by hand |
| 9,5 - 10,0 | gray claystone, easy to break down by hammer |
| 10,0 - 10,5 | browngray layer of clastic sediment, breaking down by hand to soil character |
| 10.5 | layer of harder claystone |
| 10,5 - 11,0 | light gray sediment of claystone character, easy to break down by hand, some harder positions |
| 11,0 - 11,6 | layer of soft gray claystone, in some places easy to break down by hand to soli character |
| 11,6 - 12,0 | harder fragments of gray claystone |

## GEO5 Analysis

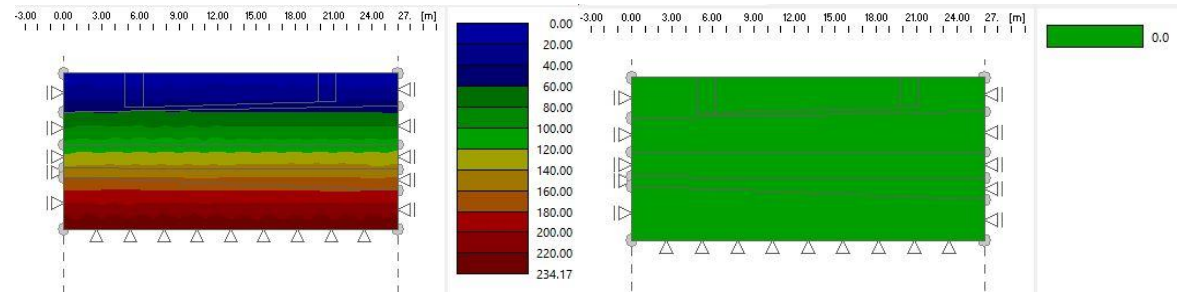


Figure 31. Stage 1 - Stress z[kPa] and Displacements [mm]

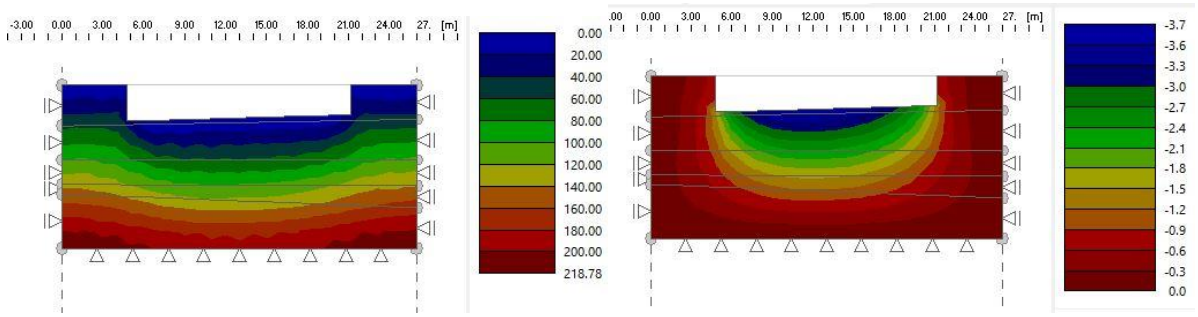


Figure 32. Stage 2 - Stress z[kPa] and Displacements [mm]

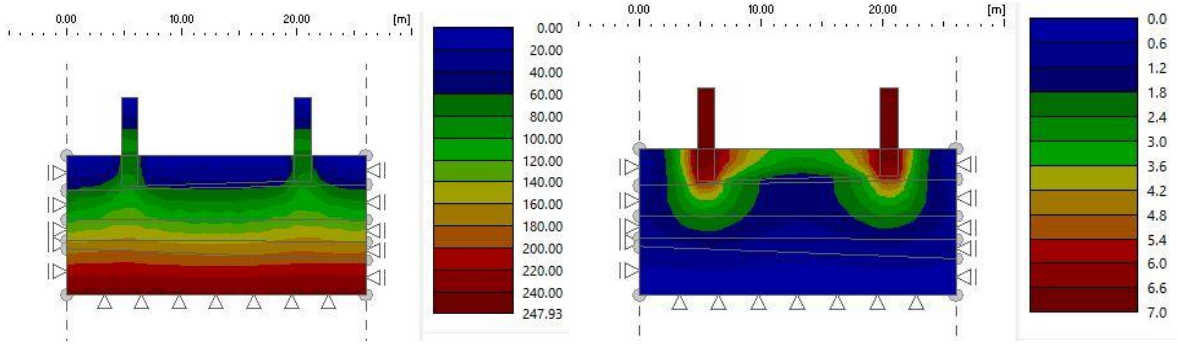


Figure 33. Stage 3 - Stress z[kPa] and Displacements [mm]

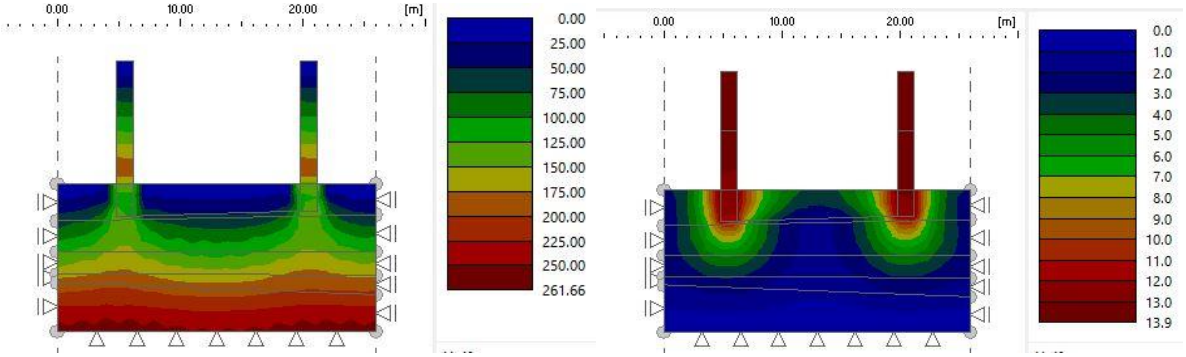


Figure 34. Stage 4 - Stress z[kPa] and Displacements [mm]

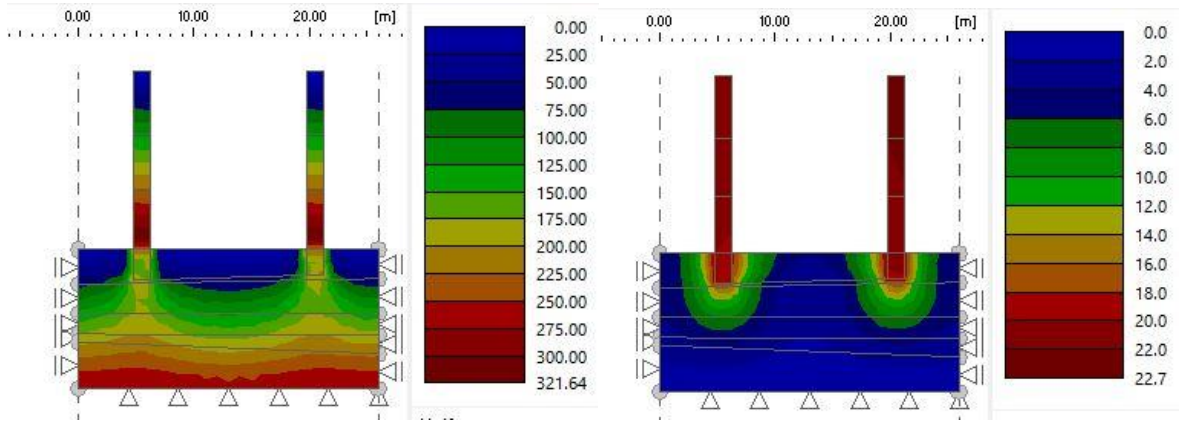


Figure 35. Stage 5 - Stress z[kPa] and Displacements [mm]

# APPENDIX D - 3D ANALYSIS - DIFFERENTIAL SOIL SETTLEMENTS

- **Area S1**

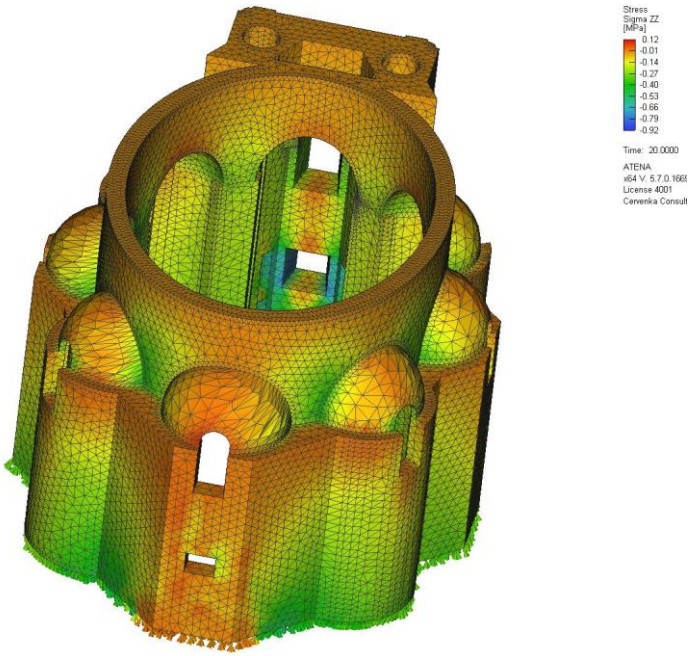


Figure 36. Stress Sigmayy

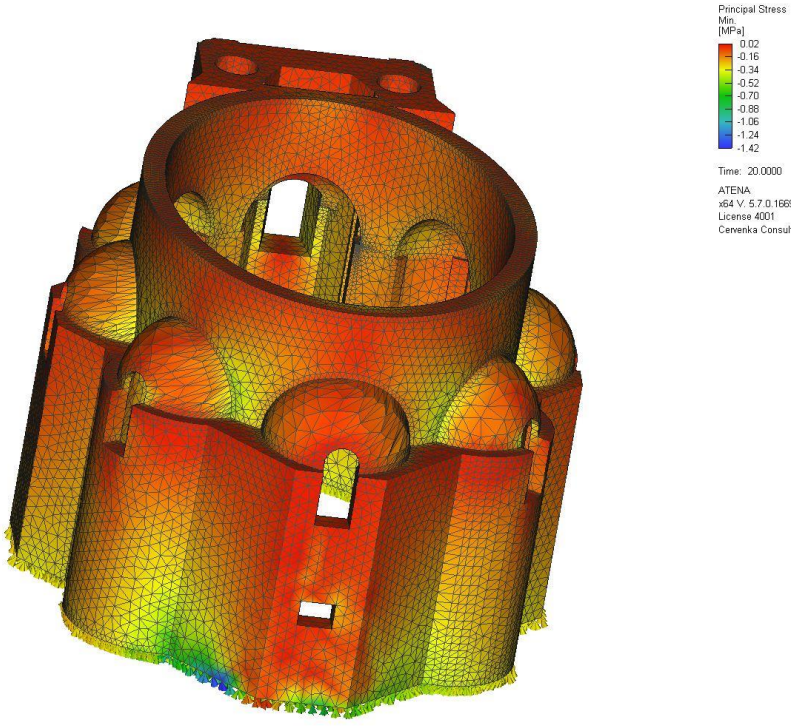


Figure 37. Principal stress Min

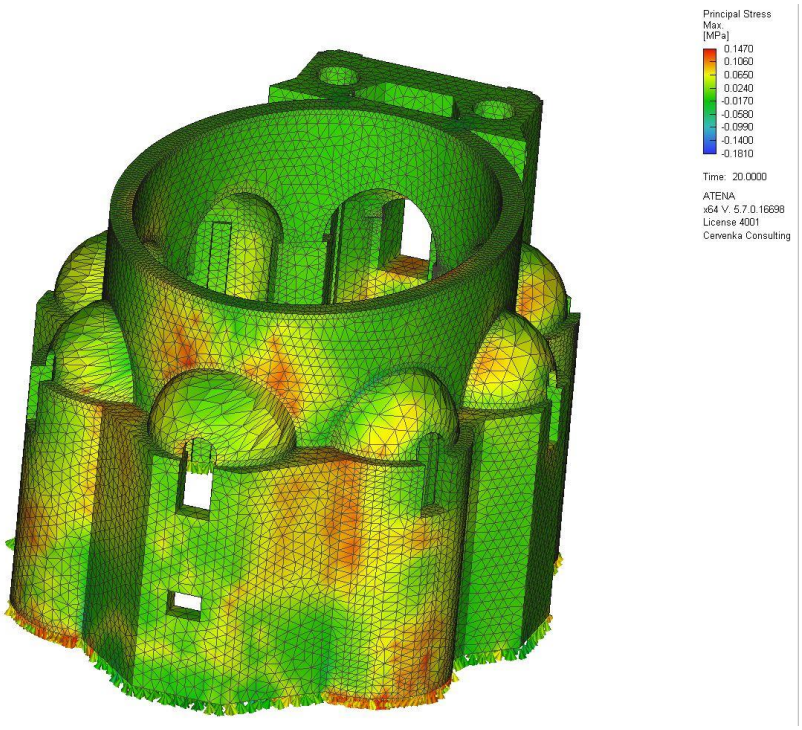


Figure 38. Principal stress min

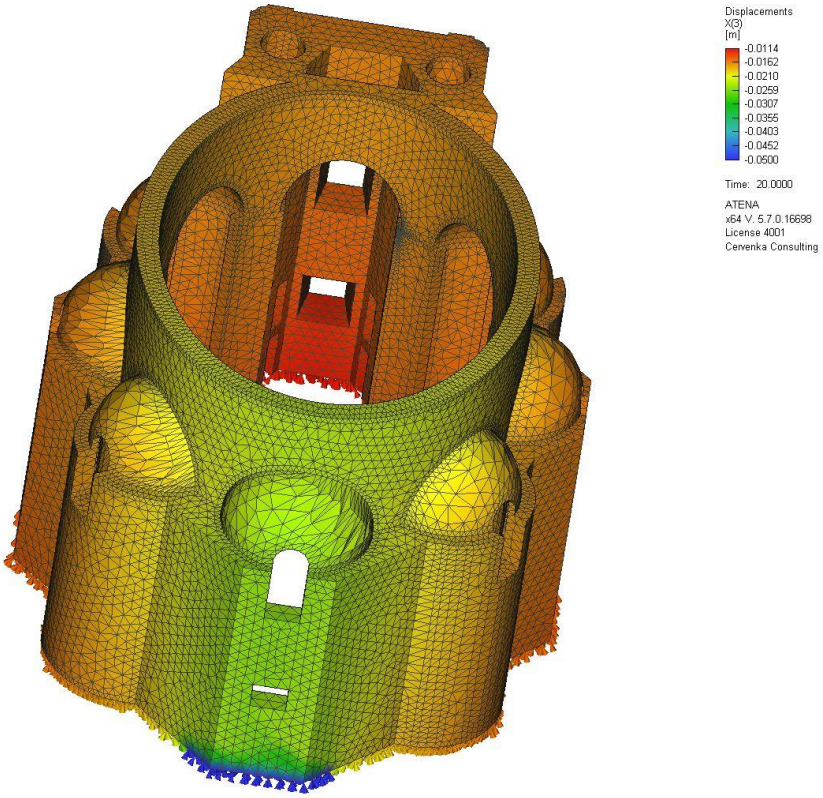


Figure 39. Displacements

- **Area S2**

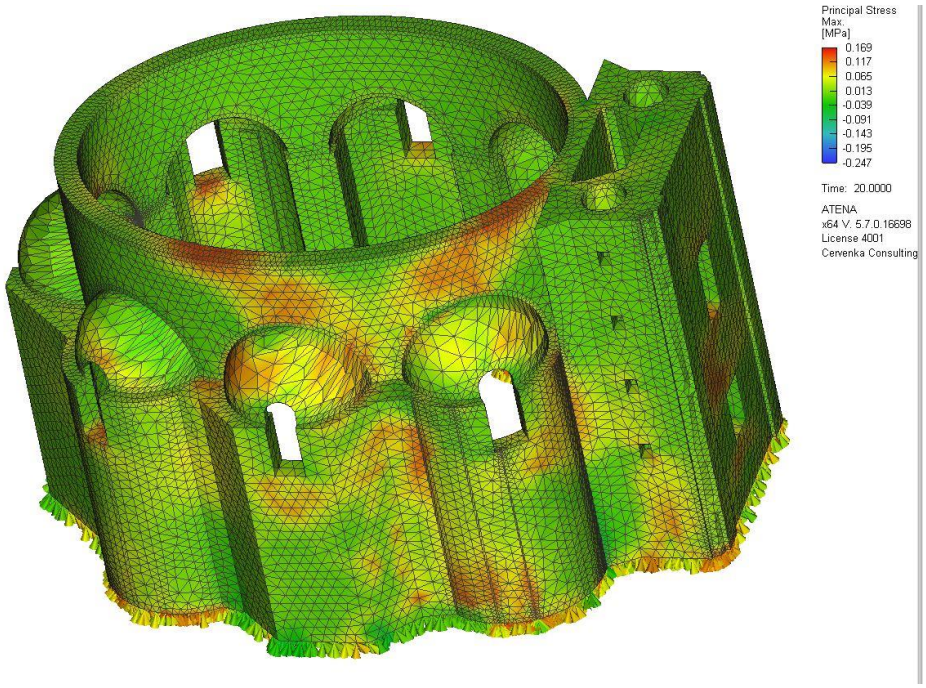


Figure 40. Principal Stress Max

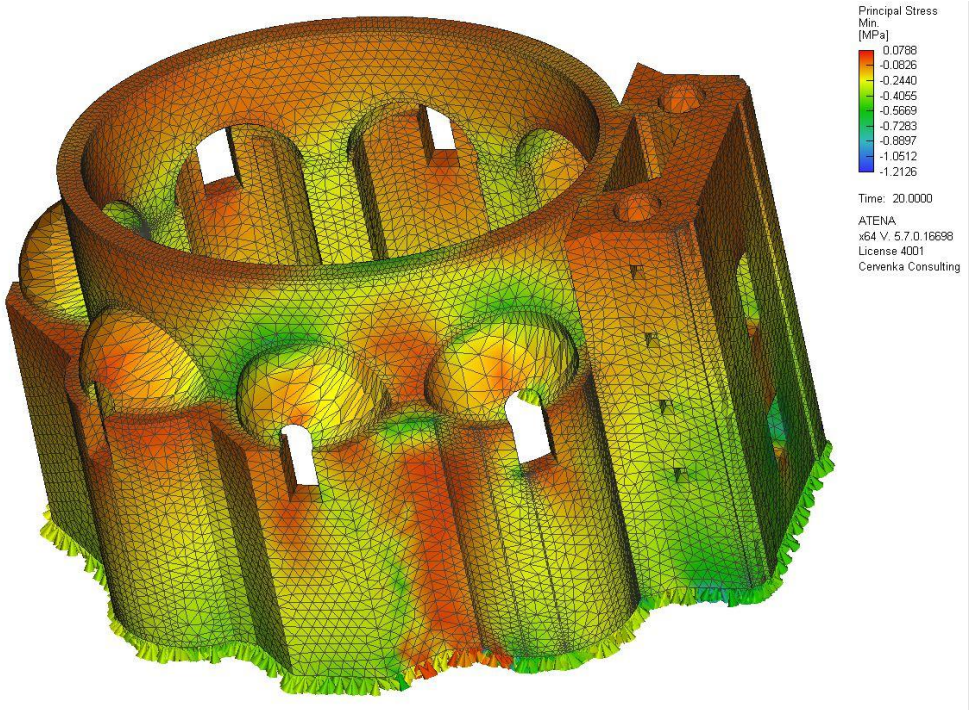


Figure 41. Principal Stress min

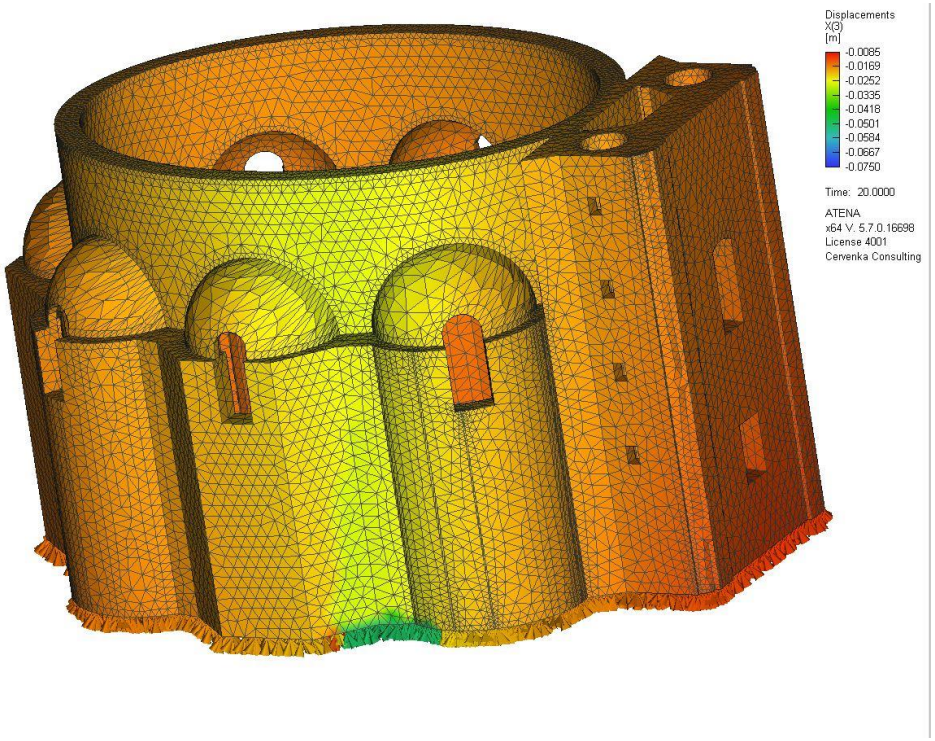


Figure 42. Displacements

- **Area S3**

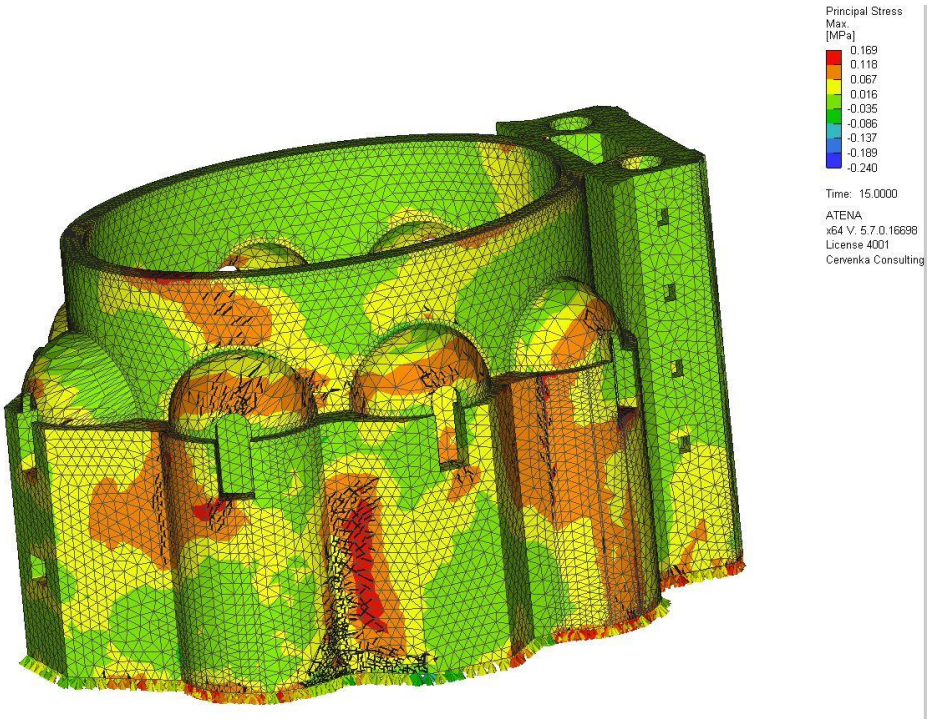


Figure 43. Principal Stress Max

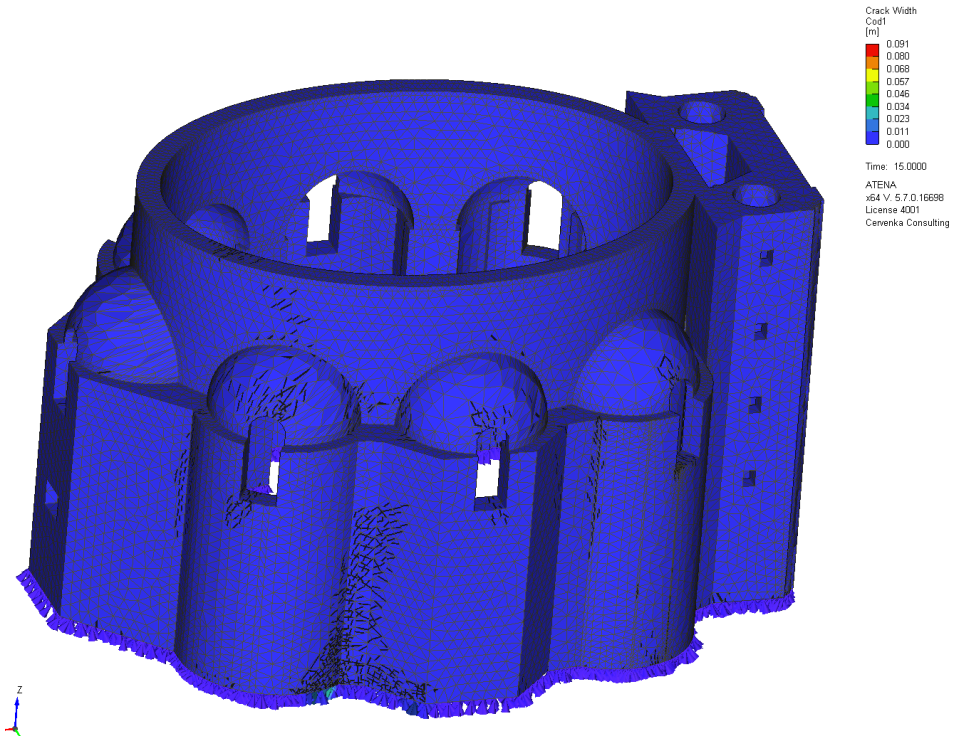


Figure 44. Crack Width